

**Figure 2**  $\alpha$ -Synuclein pathology in fibril-injected mice brain was immunoreactive for ubiquitin (Ub) and p62. (A) Staining of dentate gyrus and amygdala of fibril-injected mice at 15 months after injection, using anti-ubiquitin (upper) and p62 (lower) antibodies. Abundant ubiquitin- and p62-positive pathology can be seen. (B and C) Double-labelled immunofluorescence of dentate gyrus for phosphorylated  $\alpha$ -synuclein (Psyn) and ubiquitin (B) or p62 (C). Phosphorylated  $\alpha$ -synuclein-positive structures were co-localized with ubiquitin and p62.

interestingly, anti-mouse  $\alpha$ -synuclein strongly labelled the sarkosyl-insoluble phosphorylated  $\alpha$ -synuclein-positive bands at Day 90, but these were not immunostained with LB509. These results clearly show that endogenous mouse  $\alpha$ -synuclein is accumulated as phosphorylated and ubiquitinated forms. Immunohistochemical analysis with anti-tyrosine hydroxylase suggested that dopaminergic neurons are retained in substantia nigra of human  $\alpha$ -synuclein fibril-injected mice at 6 months after injection (Fig. 5A and B). However, dramatic loss of the neurotransmitter enkephalin was observed in globus pallidus and amygdala central nucleus, where abundant phosphorylated  $\alpha$ -synuclein-positive structures are detected (Fig. 5C and D). These data suggest that neuronal dysfunction occurs without apparent neuronal loss. We also performed behavioural analyses of mice injected with soluble human  $\alpha$ -synuclein monomers or human  $\alpha$ -synuclein fibrils. However, significant differences were not observed in open field test, wire hang test, rotarod test and Y-maze test (Supplementary Fig. 4) at 6 months after injection.

Next, we tested whether fibrils composed of recombinant mouse  $\alpha$ -synuclein can induce  $\alpha$ -synuclein pathology more efficiently than those composed of human  $\alpha$ -synuclein, because the sequences of human and mouse  $\alpha$ -synuclein are slightly different (Supplementary Fig. 5), and there could be a species difference. Mouse  $\alpha$ -synuclein complementary DNA was cloned, and the protein was expressed in *Escherichia coli* and purified. Fibrils or soluble mouse  $\alpha$ -synuclein were inoculated into substantia nigra of wild-type mouse brains and the pathology was evaluated. Strikingly, all the mice injected with mouse  $\alpha$ -synuclein fibrils developed phosphorylated  $\alpha$ -synuclein pathology in the injected side of the brain, whereas no pathology was detected in mice injected with soluble mouse  $\alpha$ -synuclein (Table 2). The phosphorylated  $\alpha$ -synuclein pathologies were basically the same as those of mice injected with human  $\alpha$ -synuclein fibrils (data not shown). The efficiency of the induction of phosphorylated  $\alpha$ -synuclein pathology by human  $\alpha$ -synuclein fibrils was  $\sim 90\%$  (Table 2), which is quite high, but slightly lower than that with mouse  $\alpha$ -synuclein fibrils, suggesting that there may be a small species difference between mouse and human  $\alpha$ -synuclein.

Finally, we tested whether pathological  $\alpha$ -synuclein deposited in the brains of patients has similar prion-like properties in brains of wild-type mice. Surprisingly, pathological  $\alpha$ -synuclein-enriched fractions also induced phosphorylated  $\alpha$ -synuclein-positive pathologies in various areas of brain, including the substantia nigra, amygdala, hippocampus, striatum, hypothalamus, somatosensory area, motor cortex, piriform cortex and superior colliculus (Fig. 6). In brains of these mice, the phosphorylated  $\alpha$ -synuclein-positive pathologies mostly resembled Lewy neurite-like structures. Lewy body-like pathology was detected only in amygdala and piriform cortex. The percentage of mice that developed phosphorylated  $\alpha$ -synuclein pathology in the injected side of the brains was 50% in the group injected with insoluble phosphorylated  $\alpha$ -synuclein of dementia with Lewy bodies brains, which is less than that in mice injected with recombinant  $\alpha$ -synuclein fibrils (Table 2). Thus, these results demonstrate that inoculation of either pure synthetic recombinant  $\alpha$ -synuclein fibrils or dementia with Lewy bodies brain extracts into wild-type mice can induce Lewy body/neurite-like phosphorylated  $\alpha$ -synuclein pathology efficiently and reproducibly. Our results raise an important question, i.e. whether or not  $\alpha$ -synuclein fibrils are transmissible among individuals. To test this possibility, we intranasally administered at high concentration of abnormal  $\alpha$ -synuclein fibrils (performed recombinant human or mouse  $\alpha$ -synuclein fibrils) or the insoluble fraction from dementia with Lewy bodies brain to normal mice. However, no pS129-positive abnormal structures were detected in the brain at 21 months after the final administration (Supplementary Fig. 6), even with highly sensitive immunohistochemical staining, suggesting that the abnormal  $\alpha$ -synuclein cannot pass through the nasal mucosa.

## Discussion

In this study, we have shown that the inoculation of  $\alpha$ -synuclein fibrils made of recombinant  $\alpha$ -synuclein or dementia with Lewy bodies brain extracts into wild-type mouse brain is sufficient to

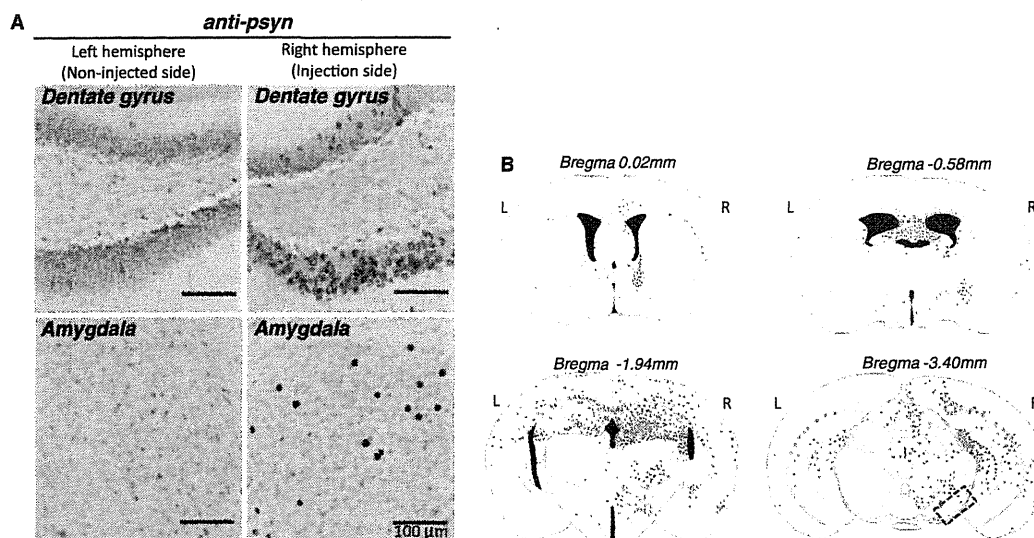


**Figure 3** (A) Spreading of phosphorylated  $\alpha$ -synuclein pathology on the contralateral side of mouse brain injected with  $\alpha$ -synuclein fibrils. Staining of dentate gyrus and amygdala in the right hemisphere (injection side) and in the left hemisphere (non-injected side) with anti-phosphorylated  $\alpha$ -synuclein (psyn) antibody, 1175, at 15 months after injection. (B) Distribution of phosphorylated  $\alpha$ -synuclein pathology in human  $\alpha$ -synuclein fibril-injected mouse brain at 15 months after injection ( $n = 24$ ). Four coronal sections were stained with phosphorylated  $\alpha$ -synuclein antibody, 1175. Red dots indicates Lewy bodies- and Lewy neurites-like pathology. Near the injection level (bregma -3.40 mm), abundant phosphorylated  $\alpha$ -synuclein pathology was present in substantia nigra, hippocampus, external capsule, and entorhinal cortex in right hemisphere, whereas in the left hemisphere, sparser pathology was detected in hippocampus and external capsule. At the level of -1.94 mm from bregma, severe phosphorylated  $\alpha$ -synuclein pathology was present in hippocampus, amygdala, corpus callosum, hypothalamus and motor, visual, somatosensory, auditory and piriform cortex in the right hemisphere, whereas moderate phosphorylated  $\alpha$ -synuclein pathology was observed in corpus callosum, hippocampus, external capsule and motor, somatosensory and auditory cortex in the left hemisphere. At the level of -0.58 mm from bregma, phosphorylated  $\alpha$ -synuclein pathology was detected in amygdala, corpus callosum, fimbria, fornix, hypothalamus, striatum and somatosensory and piriform cortex in the right hemisphere, whereas in the left hemisphere, the pathology was present in corpus callosum, fimbria, fornix, hypothalamus and striatum. At the level of 0.02 mm from bregma, phosphorylated  $\alpha$ -synuclein pathology was concentrated in stria terminalis, septal nucleus and cingulate, motor and somatosensory cortex in the right hemisphere. In the left hemisphere, phosphorylated  $\alpha$ -synuclein pathology was detected only in septal nucleus. Dashed box indicates substantia nigra (injection site). L = left hemisphere of brain; R = right hemisphere.

cause the appearance of Lewy body/neurite-like  $\alpha$ -synuclein pathology *in vivo*. Similar work was recently published by Luk *et al.* (2012a) but there are important differences between our study and theirs. Luk *et al.* (2012a) showed that only inoculation of synthetic mouse  $\alpha$ -synuclein fibrils into wild-type mouse brain induced synuclein pathology. In our present study, we inoculated not only fibrils made of recombinant mouse  $\alpha$ -synuclein but also ones from human  $\alpha$ -synuclein fibrils, and importantly also insoluble  $\alpha$ -synuclein from dementia with Lewy bodies brains, into wild-type mouse brain. This is the first report showing efficient induction of  $\alpha$ -synuclein pathology by inoculation of material from human brain. Furthermore, our biochemical analyses clearly demonstrate that endogenous mouse  $\alpha$ -synuclein is converted into abnormal form and deposited in neurons of the brain through a prion-like mechanism or by seed-dependent aggregation by crossing the species barrier (Fig. 4). Since soluble  $\alpha$ -synuclein never induced such pathology (Supplementary Fig. 2), we can conclude that the structural difference between soluble and filamentous forms of  $\alpha$ -synuclein, i.e. cross- $\beta$  structure in the  $\alpha$ -synuclein fibrils (Serpell *et al.*, 2000) is critical for the pathogenesis. It has been reported that recombinant  $\alpha$ -synuclein fibrils enhance the initiation

and progression of  $\alpha$ -synuclein pathology in transgenic mice over-expressing mutant  $\alpha$ -synuclein (Mougenot *et al.*, 2012; Luk *et al.*, 2012b) and wild-type mice (Luk *et al.*, 2012a). In those models,  $\alpha$ -synuclein pathology appeared at 90 days after inoculation. In our mouse model, abnormal phosphorylated  $\alpha$ -synuclein pathology was also detected at 90 days after injection (Fig. 4 and Table 1), suggesting that it takes about this length of time for the formation of abnormal phosphorylated  $\alpha$ -synuclein pathology *in vivo* after the seeding procedure. Despite a diffusion of injected exogenous  $\alpha$ -synuclein fibrils to the bilateral sides of brain within a few hours after injection (Fig. 4), phosphorylated  $\alpha$ -synuclein pathology seems to be initiated in the injected side and to spread from the injected side to the non-injected side in a time-dependent manner (Table 1). Thus, it is reasonable to speculate that exogenous fibrils enter neurons at the injection site as a result of infusion pressure, a temporary high concentration, or some other mechanism, and then the pathological process starts to develop from these cells.

Propagation patterns of pathology in the inoculated mice were basically identical regardless of the species of injected seeds (i.e. recombinant human  $\alpha$ -synuclein fibrils, mouse  $\alpha$ -synuclein fibrils or

Table 1 Semi-quantitative grading of  $\alpha$ -synuclein pathology in mice injected with human  $\alpha$ -synuclein fibrils

			Non-injection side (left hemisphere)			Injection side (right hemisphere)		
			Time from injection (days)			Time from injection (days)		
			90	180	450	90	180	450
Bregma	0.02 mm	Stria terminalis	–	–	–	–	++	+++
		Striatum	–	+	+	+	++	++
		Cingular cortex	–	–	–	–	+	+
		Septal nucleus	–	–	–	–	+	+
Bregma	–0.58 mm	Corpus callosum	–	–	+	–	–	++
		Fornix	–	+	++	–	+	++
		Hippocampal commissure	–	+	++	–	+	++
		Amygdala	–	–	–	+	+++	+++
		Globus pallidus	–	+	+	–	+	++
		Striatum	–	–	+	+	+	+
		Somatosensory area	–	–	+	–	+	+
		Insular cortex	–	–	–	+	+	+
Bregma	–1.94 mm	Corpus callosum	–	–	++	–	–	++
		Hippocampus	–	+	+++	+	++	+++
		Habenular nucleus	–	–	+	–	–	+++
		Fimbria	–	+	+++	–	+	+++
		Amygdala	–	–	–	++	+++	+++
		Hypothalamus	–	–	+	+	+	++
		Thalamus	–	–	–	–	–	+
		Visual cortex	–	–	+	–	+	++
		Somatosensory area	–	+	+	–	+	++
		Auditory cortex	–	–	+	+	+	++
		Piriform cortex	–	–	+	+	+	++
		External capsule	–	–	+	–	–	++
		Bregma	–3.40 mm	Substantia nigra	–	–	–	+
Hippocampus	–			+	++	+	++	++
Superior colliculus	–			+	+	–	+	++
External capsule	–			–	+	–	–	+
Visual cortex	–			–	–	+	+	+
Auditory cortex	+			+	+	+	++	++
Entorhinal cortex	–			+	+	+	++	++

Four coronal sections were stained with anti-phosphorylated  $\alpha$ -synuclein antibody at 90, 180 or 450 days after injection. Grading of  $\alpha$ -synuclein pathology was performed as follows: –, none; +, slight; ++, moderate; +++, severe. At 90 days after injection, small amounts of phosphorylated  $\alpha$ -synuclein-positive structures were observed in substantia nigra, amygdala, striatum, hypothalamus, hippocampus, and stria terminalis in the right hemisphere of brain (injected side), but very few Lewy neurites were detected in cortex in the left hemisphere. At 180 days post-injection, the amount of phosphorylated  $\alpha$ -synuclein-positive pathology was increased and was more widely spread in the right hemisphere, while in the left hemisphere, little phosphorylated  $\alpha$ -synuclein pathology was apparent in hypothalamus, hippocampus, striatum or globus pallidus. At 450 days (15 months) after injection, phosphorylated  $\alpha$ -synuclein pathology had spread throughout the right hemisphere and the left hemisphere.

dementia with Lewy bodies brain extracts), but extracts of brains with dementia with Lewy bodies showed lower propagation efficiency than recombinant fibrils (Table 2). This relatively low efficiency may be explained by the lesser amount of abnormal  $\alpha$ -synuclein contained in the dementia with Lewy bodies brain extracts. Comparison of human  $\alpha$ -synuclein fibrils and mouse  $\alpha$ -synuclein fibrils indicated that mouse  $\alpha$ -synuclein fibrils showed slightly higher efficiency (Table 2). *In vitro* experiments also indicated that mouse  $\alpha$ -synuclein fibrils promote fibrillization of the soluble mouse  $\alpha$ -synuclein monomer faster than human  $\alpha$ -synuclein fibrils (Supplementary Fig. 7). It is well known that prion propagation can cross the species barrier (Prusiner, 1993) and the efficiency of propagation depends on the amino acid sequences of prion proteins. In the case of  $\alpha$ -synuclein, mouse  $\alpha$ -synuclein and human  $\alpha$ -synuclein share 95% amino acid

sequence homology (Supplementary Fig. 5), and this may be the reason why endogenous mouse  $\alpha$ -synuclein is capable of aggregation by inoculation of human  $\alpha$ -synuclein fibrils. Another factor may be that mouse  $\alpha$ -synuclein protein has a threonine residue at amino acid position 53 (Supplementary Fig. 5), which is known as an aggregation-prone mutation in familial Parkinson's disease (Polymeropoulos *et al.*, 1997).

Time course analyses of the pathology in these mice (Table 1) showed that at 90 days after injection, phosphorylated  $\alpha$ -synuclein pathology was mainly observed near the injection level, but also seen in striatum, amygdala, stria terminalis and dentate gyrus: areas far from the injection site had developed pathology. The striatum and the amygdala central nucleus have projections from substantia nigra, and the stria terminalis serves as a major output pathway of the amygdala (Supplementary Fig. 8). Although the

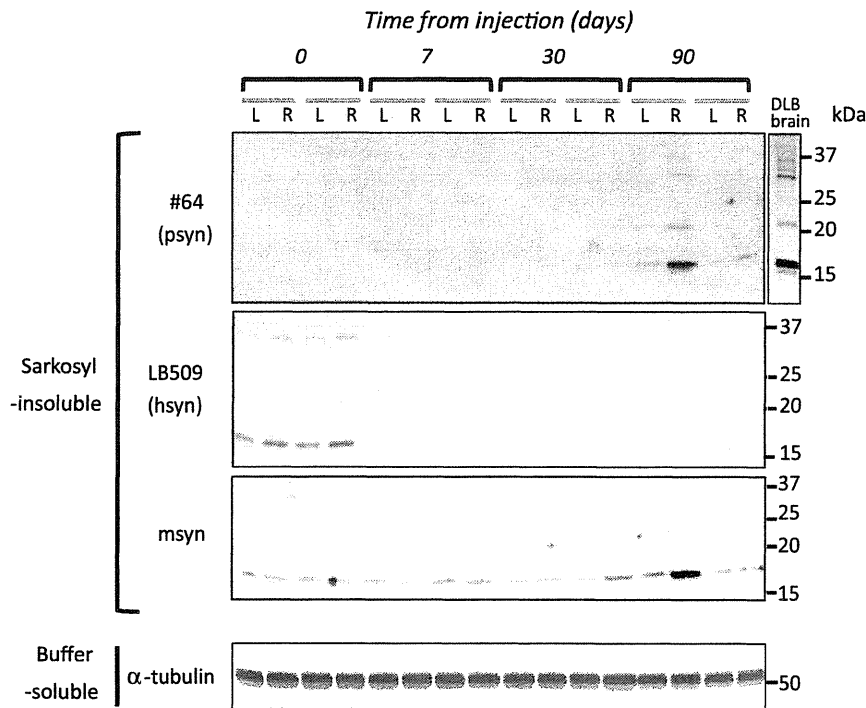


**Figure 4** Endogenous mouse  $\alpha$ -synuclein was aggregated in wild-type mouse brain injected with human  $\alpha$ -synuclein (hsyn) fibrils. The brain was divided into two parts at the longitudinal fissure of the cerebrum. Sarkosyl-insoluble fractions were obtained from the right and left hemispheres, and analysed by immunoblotting with #64, LB509 or anti-mouse  $\alpha$ -synuclein (msyn) antibodies. Representative images are shown ( $n = 14$ ). Sarkosyl-insoluble phosphorylated  $\alpha$ -synuclein (psyn) started to accumulate, predominantly in the right hemisphere, at 90 days after injection. It was composed of endogenous mouse  $\alpha$ -synuclein, not exogenous human  $\alpha$ -synuclein.

dentate gyrus does not have direct projection to substantia nigra, regions connecting with dentate gyrus (i.e., hippocampal CA1, CA3, entorhinal cortex, fimbria, fornix and hippocampal commissure) also showed moderate pathology (Table 1). These results may indicate that  $\alpha$ -synuclein pathology propagates unidirectionally through the neural circuit (Supplementary Fig. 8). Spread of pathology from the right hemisphere to the left hemisphere might occur via the corpus callosum, hippocampal commissure, etc., connecting with the contralateral side of the brain (Fig. 3B and Table 1). Phosphorylated  $\alpha$ -synuclein pathology in our mouse model was mainly observed in neurons and was hardly detected in glial cells, while the band pattern of sarkosyl-insoluble phosphorylated  $\alpha$ -synuclein in mice was indistinguishable from that of dementia with Lewy bodies brains (Fig. 4), where phosphorylated  $\alpha$ -synuclein pathology was mainly seen in neurons. Although the mechanism remains to be clarified, exogenous  $\alpha$ -synuclein fibrils may enter cells through a selective mechanism(s), such as neuron-specific receptors. Alternatively, differences in expression levels of endogenous  $\alpha$ -synuclein or cellular environments may also be important for formation of the pathology, even if abnormal  $\alpha$ -synuclein has already entered the cells.

Luk *et al.* (2012a) reported dopaminergic neuronal loss and motor dysfunction (by Rotarod test and wire hang test) in wild-type mice injected with mouse  $\alpha$ -synuclein fibrils at 6 months after inoculation into striatum. In contrast, our human  $\alpha$ -synuclein or mouse  $\alpha$ -synuclein fibril-injected mice did not

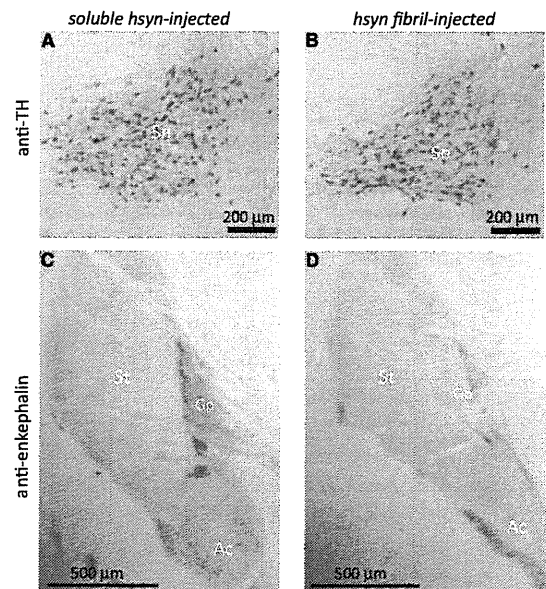


**Figure 5** Fibril-injected mice show apparent reduction of a neurotransmitter enkephalin in amygdala central nucleus and globus pallidus at 15 months after injection. Brain sections were stained with anti-tyrosine hydroxylase (TH) (A and B) and anti-enkephalin (C and D) antibodies. Ac = amygdala central nucleus; Gp = globus pallidus; Sn = substantia nigra; St = striatum.

**Table 2 Comparison of propagation efficiency in mice at 15 months after injection**

Injection samples		Right hemisphere (injection side)			Left hemisphere (non-injected side)
		anti-psyn	anti-ubiquitin	anti-p62	anti-psyn
Soluble human $\alpha$ -syn	(n = 8)	0/8 (0%)	0/8 (0%)	0/8 (0%)	0/8 (0%)
Insoluble human $\alpha$ -syn fibril	(n = 24)	22/24 (91.6%)	21/24 (87.5%)	22/24 (91.6%)	19/24 (79.2%)
Soluble mouse $\alpha$ -syn	(n = 4)	0/4 (0%)	0/4 (0%)	0/4 (0%)	0/4 (0%)
Insoluble mouse $\alpha$ -syn fibril	(n = 8)	8/8 (100%)	7/8 (87.5%)	8/8 (100%)	8/8 (100%)
DLB brain extracts	(n = 14)	7/14 (50%)	0/14 (0%)	5/14 (35.7%)	1/14 (7.1%)

In the right hemisphere, mice showing immunopositive structures for anti-phosphorylated  $\alpha$ -synuclein (psyn), ubiquitin (Ub) or p62 were counted. In the left hemisphere, mice showing immunopositive structures for anti-phosphorylated  $\alpha$ -synuclein were counted. Values show number of immunopositive mice/total mice, with percentage of immunopositive mice. DLB = dementia with Lewy bodies.

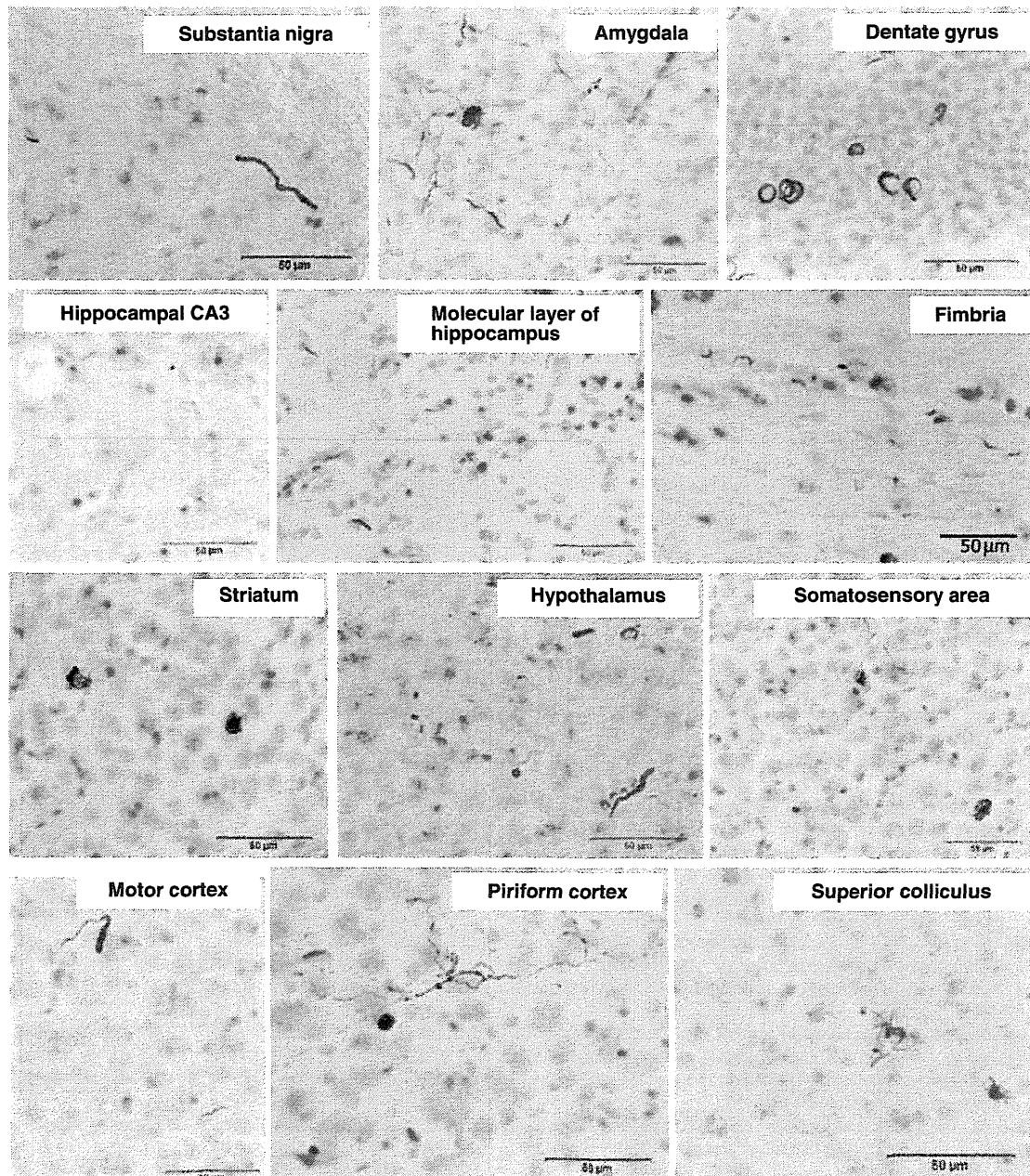


**Figure 6**  $\alpha$ -Synuclein pathology in wild-type mice brain injected with dementia with Lewy bodies-insoluble fraction observed at 15 months after injection. Sections were immunostained with anti-phosphorylated  $\alpha$ -synuclein antibody, 1175.

show any motor and cognitive deficits at 6 months after inoculation and dopaminergic degeneration even after 15 months, a dramatic reduction of enkephalin was observed in the amygdala central nucleus and globus pallidus, with severe pathology, at 6 months after injection (Fig. 5 and Supplementary Fig. 4). The different phenotypes of these mice might be explained by differences in the injection sites [striatum in Luk *et al.* (2012a) and substantia nigra in our study]. Nonetheless, the spreading pattern of the pathological  $\alpha$ -synuclein is different between our study and theirs. Differential vulnerability of neurons to these abnormal proteins may also affect phenotypes of these mice.

In summary, we have shown that intracerebral injection of insoluble  $\alpha$ -synuclein fibrils can induce aggregation of endogenous mouse  $\alpha$ -synuclein through a prion-like propagation mechanism. Our data suggest that phosphorylated  $\alpha$ -synuclein pathologies do not induce acute neuronal loss but induce a slow neurodegeneration by disrupting neuronal function. These models should be useful not only for elucidating the molecular mechanisms of propagation of intracellular abnormal proteins, but also for development and evaluation of disease-modifying therapy.

## Funding

This work was supported by MEXT KAKENHI Grant Numbers 12937622, 12901980 (to M.H.), JSPS KAKENHI Grant Number 11024780 (to M.M.-S.) and MHLW Grant Number 12946221 (to M.H.).

## Supplementary material

Supplementary material is available at *Brain* online.

## References

- Baba M, Nakajo S, Tu PH, Tomita T, Nakaya K, Lee VM, et al. Aggregation of alpha-synuclein in Lewy bodies of sporadic Parkinson's disease and dementia with Lewy bodies. *Am J Pathol* 1998; 152: 879–84.
- Braak H, Braak E. Neuropathological staging of Alzheimer-related changes. *Acta Neuropathol* 1991; 82: 239–59.
- Chartier-Harlin MC, Kachergus J, Roumier C, Mouroux V, Douay X, Lincoln S, et al. Alpha-synuclein locus duplication as a cause of familial Parkinson's disease. *Lancet* 2004; 364: 1167–9.
- Clavaguera F, Bolmont T, Crowther RA, Abramowski D, Frank S, Probst A, et al. Transmission and spreading of tauopathy in transgenic mouse brain. *Nat Cell Biol* 2009; 11: 909–13.
- Desplats P, Lee HJ, Bae EJ, Patrick C, Rockenstein E, Crews L, et al. Inclusion formation and neuronal cell death through neuron-to-neuron transmission of alpha-synuclein. *Proc Natl Acad Sci USA* 2009; 106: 13010–5.
- Emmanouilidou E, Melachroinou K, Roumeliotis T, Garbis SD, Ntzouni M, Margaritis LH, et al. Cell-produced alpha-synuclein is secreted in a calcium-dependent manner by exosomes and impacts neuronal survival. *J Neurosci* 2010; 30: 6838–51.
- Fujiwara H, Hasegawa M, Dohmae N, Kawashima A, Masliah E, Goldberg MS, et al. Alpha-Synuclein is phosphorylated in synucleinopathy lesions. *Nat Cell Biol* 2002; 4: 160–4.
- Goedert M. Alpha-synuclein and neurodegenerative diseases. *Nat Rev Neurosci* 2001; 2: 492–501.
- Ibanez P, Bonnet AM, Debarges B, Lohmann E, Tison F, Pollak P, et al. Causal relation between alpha-synuclein gene duplication and familial Parkinson's disease. *Lancet* 2004; 364: 1169–71.
- Kordower JH, Chu Y, Hauser RA, Freeman TB, Olanow CW. Lewy body-like pathology in long-term embryonic nigral transplants in Parkinson's disease. *Nat Med* 2008; 14: 504–6.
- Kruger R, Kuhn W, Muller T, Woitalla D, Graeber M, Kosel S, et al. Ala30Pro mutation in the gene encoding alpha-synuclein in Parkinson's disease. *Nat Genet* 1998; 18: 106–8.
- Kuusisto E, Salminen A, Alafuzoff I. Ubiquitin-binding protein p62 is present in neuronal and glial inclusions in human tauopathies and synucleinopathies. *Neuroreport* 2001; 12: 2085–90.
- Li JY, Englund E, Holton JL, Soulet D, Hagell P, Lees AJ, et al. Lewy bodies in grafted neurons in subjects with Parkinson's disease suggest host-to-graft disease propagation. *Nat Med* 2008; 14: 501–3.
- Luk KC, Kehm V, Carroll J, Zhang B, O'Brien P, Trojanowski JQ, et al. Pathological alpha-synuclein transmission initiates Parkinson-like neurodegeneration in nontransgenic mice. *Science* 2012a; 338: 949–53.
- Luk KC, Kehm VM, Zhang B, O'Brien P, Trojanowski JQ, Lee VM. Intracerebral inoculation of pathological alpha-synuclein initiates a rapidly progressive neurodegenerative alpha-synucleinopathy in mice. *J Exp Med* 2012b; 209: 975–86.
- Masuda M, Dohmae N, Nonaka T, Oikawa T, Hisanaga S, Goedert M, et al. Cysteine misincorporation in bacterially expressed human alpha-synuclein. *FEBS Lett* 2006a; 580: 1775–9.
- Masuda M, Suzuki N, Taniguchi S, Oikawa T, Nonaka T, Iwatsubo T, et al. Small molecule inhibitors of alpha-synuclein filament assembly. *Biochemistry* 2006b; 45: 6085–94.
- Mougenot AL, Nicot S, Bencsik A, Morignat E, Verchere J, Lakhdar L, et al. Prion-like acceleration of a synucleinopathy in a transgenic mouse model. *Neurobiol Aging* 2012; 33: 2225–8.
- Muller CM, de Vos RA, Maurage CA, Thal DR, Tolnay M, Braak H. Staging of sporadic Parkinson disease-related alpha-synuclein pathology: inter- and intra-rater reliability. *J Neuropathol Exp Neurol* 2005; 64: 623–8.
- Nonaka T, Kametani F, Arai T, Akiyama H, Hasegawa M. Truncation and pathogenic mutations facilitate the formation of intracellular aggregates of TDP-43. *Hum Mol Genet* 2009; 18: 3353–64.
- Nonaka T, Watanabe ST, Iwatsubo T, Hasegawa M. Seeded aggregation and toxicity of {alpha}-synuclein and tau: cellular models of neurodegenerative diseases. *J Biol Chem* 2010; 285: 34885–98.
- Polymeropoulos MH, Lavedan C, Leroy E, Ide SE, Dehejia A, Dutra A, et al. Mutation in the alpha-synuclein gene identified in families with Parkinson's disease. *Science* 1997; 276: 2045–7.
- Prusiner SB. Genetic and infectious prion diseases. *Arch Neurol* 1993; 50: 1129–53.
- Serpell LC, Berriman J, Jakes R, Goedert M, Crowther RA. Fiber diffraction of synthetic alpha-synuclein filaments shows amyloid-like cross-beta conformation. *Proc Natl Acad Sci USA* 2000; 97: 4897–902.
- Shiotsuki H, Yoshimi K, Shimo Y, Funayama M, Takamatsu Y, Ikeda K, et al. A rotarod test for evaluation of motor skill learning. *J Neurosci Methods* 2010; 189: 180–5.
- Singleton AB, Farrer M, Johnson J, Singleton A, Hague S, Kachergus J, et al. alpha-Synuclein locus triplication causes Parkinson's disease. *Science* 2003; 302: 841.
- Spillantini MG, Crowther RA, Jakes R, Hasegawa M, Goedert M. alpha-Synuclein in filamentous inclusions of Lewy bodies from Parkinson's disease and dementia with lewy bodies. *Proc Natl Acad Sci USA* 1998; 95: 6469–73.
- Spillantini MG, Schmidt ML, Lee VM, Trojanowski JQ, Jakes R, Goedert M. Alpha-synuclein in Lewy bodies. *Nature* 1997; 388: 839–40.
- Stohr J, Watts JC, Mensinger ZL, Oehler A, Grillo SK, Dearmond SJ, et al. Purified and synthetic Alzheimer's amyloid beta (Abeta) prions. *Proc Natl Acad Sci USA* 2012; 109: 11025–30.



Volpicelli-Daley LA, Luk KC, Patel TP, Tanik SA, Riddle DM, Stieber A, et al. Exogenous alpha-synuclein fibrils induce Lewy body pathology leading to synaptic dysfunction and neuron death. *Neuron* 2011; 72: 57–71.

Wakabayashi K, Yoshimoto M, Tsuji S, Takahashi H. Alpha-synuclein immunoreactivity in glial cytoplasmic inclusions in multiple system atrophy. *Neurosci Lett* 1998; 249: 180–2.

Yonetani M, Nonaka T, Masuda M, Inukai Y, Oikawa T, Hisanaga S, et al. Conversion of wild-type alpha-synuclein into mutant-type fibrils and its propagation in the presence of A30P mutant. *J Biol Chem* 2009; 284: 7940–50.

Zarranz JJ, Alegre J, Gomez-Esteban JC, Lezcano E, Ros R, Ampuero I, et al. The new mutation, E46K, of alpha-synuclein causes Parkinson and Lewy body dementia. *Ann Neurol* 2004; 55: 164–73.

# Prion-like Properties of Pathological TDP-43 Aggregates from Diseased Brains

Takashi Nonaka,<sup>1,\*</sup> Masami Masuda-Suzukake,<sup>1</sup> Tetsuaki Arai,<sup>2,3</sup> Yoko Hasegawa,<sup>1</sup> Hiroyasu Akatsu,<sup>4</sup> Tomokazu Obi,<sup>5</sup> Mari Yoshida,<sup>6</sup> Shigeo Murayama,<sup>7</sup> David M.A. Mann,<sup>8</sup> Haruhiko Akiyama,<sup>2</sup> and Masato Hasegawa<sup>1,\*</sup>

<sup>1</sup>Department of Neuropathology and Cell Biology

<sup>2</sup>Dementia Research Project

Tokyo Metropolitan Institute of Medical Science, Setagaya-ku, Tokyo 156-8506, Japan

<sup>3</sup>Division of Clinical Medicine, Department of Neuropsychiatry, Faculty of Medicine, University of Tsukuba, Tsukuba, Ibaraki 305-8575, Japan

<sup>4</sup>Choju Medical Institute, Fukushima Hospital, Toyohashi, Aichi 441-8124, Japan

<sup>5</sup>Shizuoka Institute of Epilepsy and Neurological Disorders, Shizuoka, Shizuoka 420-8688, Japan

<sup>6</sup>Institute for Medical Science of Aging, Aichi Medical University, Nagakute, Aichi 480-1195, Japan

<sup>7</sup>Department of Neuropathology, Tokyo Metropolitan Institute of Gerontology, Itabashi-ku, Tokyo 173-0015, Japan

<sup>8</sup>Centre for Clinical and Cognitive Neuroscience, Institute of Brain Behavior and Mental Health, University of Manchester, Salford M6 8HD, UK

\*Correspondence: nonaka-tk@igakuken.or.jp (T.N.), hasegawa-ms@igakuken.or.jp (M.H.)

<http://dx.doi.org/10.1016/j.celrep.2013.06.007>

This is an open-access article distributed under the terms of the Creative Commons Attribution-NonCommercial-No Derivative Works License, which permits non-commercial use, distribution, and reproduction in any medium, provided the original author and source are credited.

## SUMMARY

TDP-43 is the major component protein of ubiquitin-positive inclusions in brains of patients with frontotemporal lobar degeneration (FTLD-TDP) or amyotrophic lateral sclerosis (ALS). Here, we report the characterization of prion-like properties of aggregated TDP-43 prepared from diseased brains. When insoluble TDP-43 from ALS or FTLD-TDP brains was introduced as seeds into SH-SY5Y cells expressing TDP-43, phosphorylated and ubiquitinated TDP-43 was aggregated in a self-templating manner. Immunoblot analyses revealed that the C-terminal fragments of insoluble TDP-43 characteristic of each disease type acted as seeds, inducing seed-dependent aggregation of TDP-43 in these cells. The seeding ability of insoluble TDP-43 was unaffected by proteinase treatment but was abrogated by formic acid. One subtype of TDP-43 aggregate was resistant to boiling treatment. The insoluble fraction from cells harboring TDP-43 aggregates could also trigger intracellular TDP-43 aggregation. These results indicate that insoluble TDP-43 has prion-like properties that may play a role in the progression of TDP-43 proteinopathy.

## INTRODUCTION

Frontotemporal lobar degeneration (FTLD) and amyotrophic lateral sclerosis (ALS) are well-known neurodegenerative disorders. FTLD is the second most common form of cortical dementia in the population below the age of 65 years (Snowden et al., 2002). ALS is the most common form of motor neuron disease

and is characterized by progressive weakness and muscular wasting, and death within a few years. Ubiquitin-positive inclusions composed of misfolded proteins in neuronal and glial cells are common neuropathological features of most neurodegenerative diseases, including Alzheimer's disease (AD), Parkinson's disease (PD), FTLD, and ALS. Recently, TAR DNA-binding protein of 43 kDa (TDP-43) was identified as the major component of inclusions found in the brains of patients with ALS and FTLD (FTLD-U or FTLD-TDP) (Arai et al., 2006; Neumann et al., 2006). TDP-43, a 414-amino-acid protein expressed in nuclei, belongs to the heterogeneous ribonucleoprotein family, members of which are involved in repression of gene transcription, regulation of exon splicing, and nuclear body functions (Buratti and Baralle, 2009; Buratti et al., 2001). TDP-43 is thought to be essential for early embryonic development, because homozygous disruption of the TDP-43 gene (*TARDBP*) causes early embryonic lethality (Sephton et al., 2010; Wu et al., 2010). Interestingly, affected neurons containing cytoplasmic TDP-43 inclusions show depletion of normal nuclear TDP-43 (Arai et al., 2006; Neumann et al., 2006). Patients with these diseases show autosomal-dominant missense mutations in the *TARDBP* gene, mostly located in the C-terminal glycine-rich region (Pesiridis et al., 2009), and pathological TDP-43 is hyperphosphorylated, ubiquitinated, and abnormally cleaved to generate aggregation-prone C-terminal fragments (CTFs) (Arai et al., 2010; Hasegawa et al., 2008, 2011). Thus, loss of normal function of nuclear TDP-43 due to cytoplasmic mislocalization, and toxic gain of function due to cytoplasmic TDP-43 aggregation are potential disease mechanisms (Arai et al., 2006; Neumann et al., 2006).

Aberrant protein aggregates in affected neurons are well-known hallmarks of neurodegenerative diseases, but the mechanisms involved remain unclear. Recent reports suggest that prion-like propagation of protein aggregates composed of tau or  $\alpha$ -synuclein may be involved in progression of neurodegenerative diseases such as AD or PD. This is consistent with findings that tau- or  $\alpha$ -synuclein pathology spreads in a



stereotypical temporal and topological manner (Braak and Braak, 1991; Braak et al., 2003). Furthermore, fetal mesencephalic grafts in the striatum of PD patients eventually develop Lewy bodies, suggesting that pathologic  $\alpha$ -synuclein could be transmitted from diseased striatal neurons to grafted neurons (Kordower et al., 2008; Li et al., 2008). Cell-cell transmission of tau- and  $\alpha$ -synuclein aggregates has been observed in both cell culture and animal models (Clavaguera et al., 2009; de Calignon et al., 2012; Desplats et al., 2009; Frost et al., 2009; Goedert et al., 2010; Liu et al., 2012; Luk et al., 2009, 2012a, 2012b; Nonaka et al., 2010; Masuda-Suzukake et al., 2013). Therefore, prion-like propagation of aberrant protein aggregates may be involved in the pathogenesis of neurodegenerative diseases.

Here, we show that insoluble TDP-43 aggregates in brains of ALS and FTLD-TDP patients have prion-like properties, including the ability to seed intracellular TDP-43 aggregation, stability against heat and proteinases, and cell-to-cell transmissibility.

## RESULTS

### Intracellular TDP-43 Is Aggregated in a Seed-Dependent Manner

The C-terminal portion of TDP-43 has sequence similarity to prion (Guo et al., 2011). Therefore, to investigate whether intracellular TDP-43 is aggregated in a self-templating manner, like prion, we first established a cell culture model for seeded aggregation of intracellular TDP-43 using SH-SY5Y and 293T cells (Figures 1 and S1A).

We examined whether TDP-43 forms intracellular aggregates in the presence of insoluble TDP-43 prepared from ALS or FTLD-TDP brains as seeds. We observed filamentous structures that were positive for antiphospho TDP-43 (anti-pS409/410) antibody (10–15 nm in diameter) by electron microscopy analyses of insoluble TDP-43 from brains of patients (Figure 1A). Furthermore, it was recently reported that TDP-43 inclusions in ALS and FTLD-TDP showed thioflavin positivity (Bigio et al., 2013). These results clearly indicate that insoluble TDP-43 from brains, used as seeds, had the properties of amyloid. To distinguish plasmid-derived TDP-43 from insoluble TDP-43 introduced as seeds, we used a plasmid encoding hemagglutinin (HA)-tagged TDP-43. SH-SY5Y cells were transiently transfected with HA-tagged TDP-43 and then transduced with or without N-lauroylsarcosine sodium salt (sarkosyl)-insoluble fraction (Sar-ppt) prepared from the brains of ALS (ALS ppt) or FTLD-TDP (FTLD ppt) patients. Cell lysates were fractionated and immunoblotted with anti-HA and anti-pS409/410 antibodies. In cells transfected with HA-TDP-43 plasmid alone, expressed HA-TDP-43 was detected in all fractions with an antibody against HA, whereas phosphorylated HA-TDP-43 was modestly detected in the insoluble fraction (ppt), indicating that the transiently expressed HA-TDP-43 was slightly aggregated (Figure 1B). In cells treated with ALS ppt (5  $\mu$ g) alone, several bands were detected in ppt fractions with anti-pS409/410, suggesting that endogenous TDP-43 is aggregated in the presence of seeds. On the other hand, in HA-TDP-43-expressing cells transduced with ALS ppt (5  $\mu$ g), bands with slower mobility were seen with an antibody against HA, and both phosphorylated full-length HA-TDP-43 and its

CTFs were detected with anti-pS409/410. We confirmed that plasmid-derived TDP-43, but not ALS ppt seeds, is mainly aggregated in ppt fractions, because no bands were detected with anti-pS409/410 when ALS ppt (5  $\mu$ g, used as seeds) alone was loaded on the gel (Figure 1C, rightmost lane). Similarly, full-length HA-TDP-43 and CTFs positive for anti-pS409/410 were produced in cells transfected with both HA-TDP-43 plasmid and FTLD ppt (Figures 1B and S1B). Given that plasmid-derived, nontagged TDP-43 was accumulated intracellularly in the presence of ALS ppt (Figure 1C), we mainly used a plasmid encoding, nontagged TDP-43 in subsequent work.

To test whether insoluble TDP-43 in diseased brain extracts can function as seeds for aggregation, we prepared immunodepleted ALS ppt (Figure 1D) as seeds for intracellular TDP-43 aggregation. Sar-ppt of ALS brain was incubated with a mixture of anti-TDP-43 (polyclonal; Proteintech) and anti-pS409/410 antibodies, followed by addition of protein G-Sepharose. After overnight incubation, the supernatant fraction was analyzed by immunoblotting. As shown in Figure 1D (left panel), the immunoreactivity against anti-pS409/410 found in nontreated ALS ppt was wholly lost after immunodepletion (ID). Then, we introduced immunodepleted ALS ppt (ALS ppt ID) into cells expressing HA-TDP-43, using MultiFectam. As shown in Figure 1D (right panel), the band intensities of phosphorylated full-length HA-TDP-43 and CTFs in the ppt fraction of cells expressing HA-TDP-43 and treated with ALS ppt ID were much weaker than those in the case of cells expressing HA-TDP-43 and treated with nonimmunodepleted ALS ppt. We also tested the specificity of ALS ppt as seeds for aggregation of TDP-43. When recombinant  $\alpha$ -synuclein fibrils were introduced into cells transiently expressing  $\alpha$ -synuclein, phosphorylated  $\alpha$ -synuclein was accumulated in Triton-insoluble fractions (Figure S2A), as previously reported (Nonaka et al., 2010). However, intracellular  $\alpha$ -synuclein aggregation was not observed in cells expressing  $\alpha$ -synuclein and treated with ALS ppt (Figure S2B). Furthermore, HA-TDP-43 was not aggregated in the presence of  $\alpha$ -synuclein fibril seeds (Figure S2C). These results showed that insoluble TDP-43 functions specifically as seeds for intracellular aggregation of TDP-43, but not for aggregation of  $\alpha$ -synuclein.

We performed immunocytochemical analyses of cells expressing HA-TDP-43 and treated with or without ALS ppt. No phosphorylated and aggregated TDP-43 was seen in cells expressing HA-TDP-43 only (Figure 1E). A few dot-like structures positive for anti-pS409/410 were found in nontransfected cells treated with ALS ppt. On the other hand, round cytoplasmic inclusions of TDP-43 positive for both anti-pS409/410 and an antibody against Ub were detected in cells expressing HA-TDP-43 and treated with ALS ppt. The percentage of HA-positive cells that were also positive for anti-pS409/410 antibody was calculated to be  $11.4\% \pm 4.3\%$ . Interestingly, the immunoreactivity of an antibody against HA in nuclei of cells with cytoplasmic TDP-43 aggregates was less than that in nuclei of cells expressing HA-TDP-43 without aggregates (Figure 1E, lower left), as seen for pathogenic neurons with cytoplasmic TDP-43 inclusions in ALS and FTLD-TDP brains. Taken together, these results suggest that intracellular TDP-43 was efficiently aggregated in cultured cells in a manner that depended on seeding with insoluble TDP-43 derived from patients' brains.

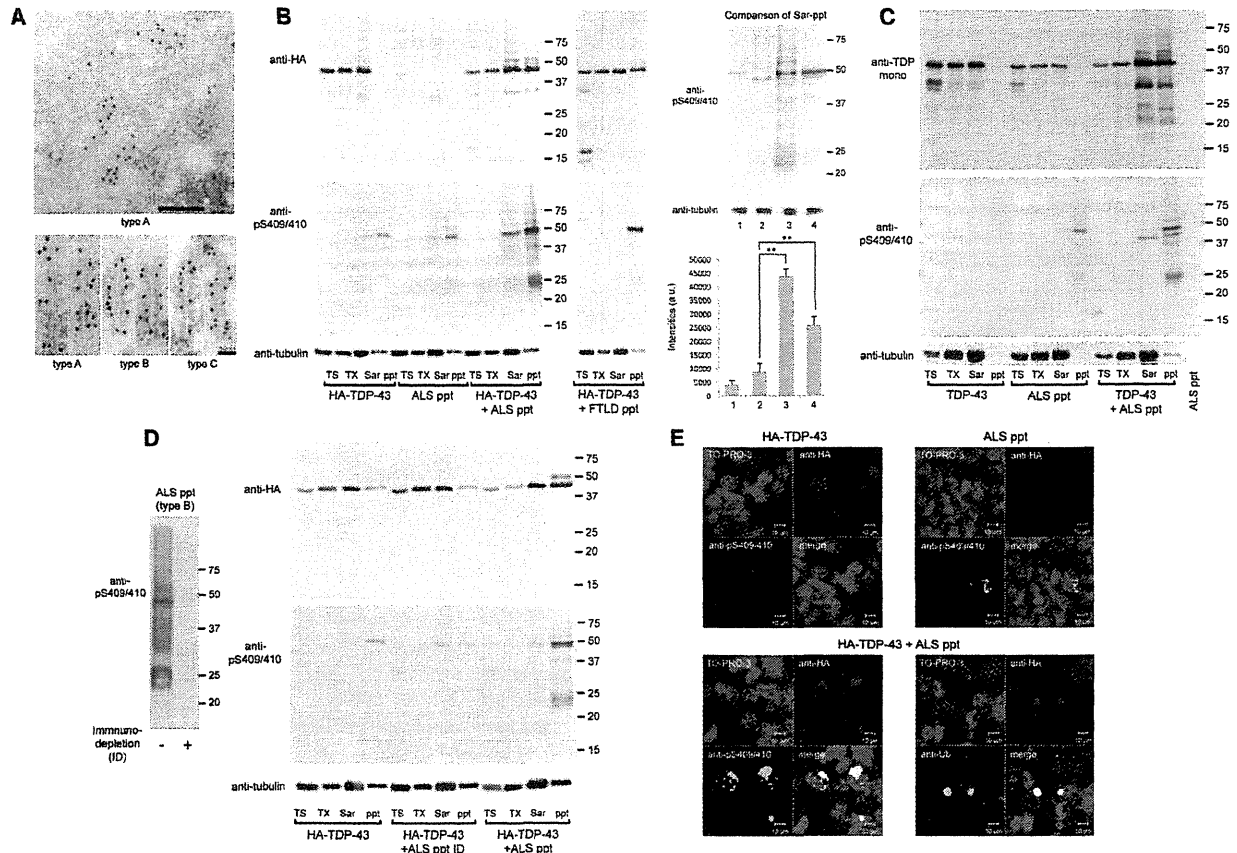


**Figure 1. Detergent-Insoluble Fractions from ALS and FTLD-TDP Brains Function as Seeds for Intracellular Aggregation of Plasmid-Derived TDP-43**

(A) Immuno-electron microscopy analyses of insoluble fractions from diseased brains (types A, B, and C). Filamentous structures are labeled with anti-phospho TDP-43 antibody (pS409/410). Scale bars represent 200 nm in upper panel, 50 nm in lower panel.

(B) Immunoblot analysis of lysates from cells expressing HA-TDP-43 plasmid only (HA-TDP-43), cells treated with ALS ppt (5  $\mu$ g; ALS ppt), cells transfected with both HA-TDP-43 and ALS ppt (HA-TDP-43 + ALS ppt), and cells transfected with both HA-TDP-43 and FTLD ppt (5  $\mu$ g; HA-TDP-43 + FTLD ppt). Proteins were differentially extracted from cells with Tris-HCl (TS), Triton X-100 (TX), and sarkosyl (Sar), leaving the pellet (ppt). Blots were probed using anti-HA (upper) and anti-pS409/410 (lower). In the right panel, the Sar-ppt fractions are shown side by side. 1: HA-TDP-43; 2: ALS ppt; 3: HA-TDP-43 + ALS ppt; 4: HA-TDP-43 + FTLD ppt. The immunoreactivity of each lane that was positive for anti-pS409/410 was quantified and the results are expressed as means  $\pm$  SEM (n = 3). \*\*p < 0.0005 by Student's t test; a.u., arbitrary unit.

See also Figure S1.

(C) Immunoblot analysis of proteins extracted from cells expressing only nontagged TDP-43 plasmid (TDP-43), cells treated only with ALS ppt (ALS ppt), and cells transfected with both TDP-43 and ALS ppt (TDP-43 + ALS ppt). Blots were probed using anti-TDP-43 monoclonal antibody (upper) and anti-pS409/410 (lower). No bands were detected when only ALS ppt (5  $\mu$ g) used as seeds was loaded on the gel (rightmost lane).

(D) ID of ALS ppt was performed with (+) or without (–) a mixture of anti-TDP-43 and anti-pS409/410 antibody. This was followed by immunoblot analyses with anti-pS409/410 (left panel). Proteins differentially extracted from cells expressing only HA-TDP-43 plasmid (HA-TDP-43), and cells transfected with both HA-TDP-43 and immunodepleted ALS ppt (HA-TDP-43 + ALS ppt ID) or untreated ALS ppt (HA-TDP-43 + ALS ppt) were analyzed. Blots were probed using anti-HA (upper) and anti-pS409/410 (lower).

(E) Confocal laser microscopy analyses of cells expressing only HA-TDP-43 plasmid (HA-TDP-43), cells treated with detergent-insoluble fraction of ALS brain (ALS ppt), and cells transfected with both HA-TDP-43 and ALS ppt (HA-TDP-43 + ALS ppt) immunostained with anti-HA (red), anti-pS409/410 (green) or anti-Ub (green), and counterstained with TO-PRO-3 (blue). Scale bars represent 10  $\mu$ m.

### Aggregation of Full-Length TDP-43 Precedes Generation of TDP-43 CTFs

To further investigate the seed-dependent intracellular aggregation of TDP-43, we performed time-course experiments and immunoblot analyses during TDP-43 aggregate formation. Cells expressing HA-TDP-43 and treated with or without ALS ppt were

incubated for 1–3 days, and each day the cell lysates were fractionated as described above. No band positive for anti-pS409/410 was detected in any fraction on day 1 or day 2, whereas a weak band of phosphorylated HA-TDP-43 was seen in the insoluble fraction (ppt) on day 3 of cells expressing HA-TDP-43 (Figure 2A). When cells were transfected with both HA-TDP-43

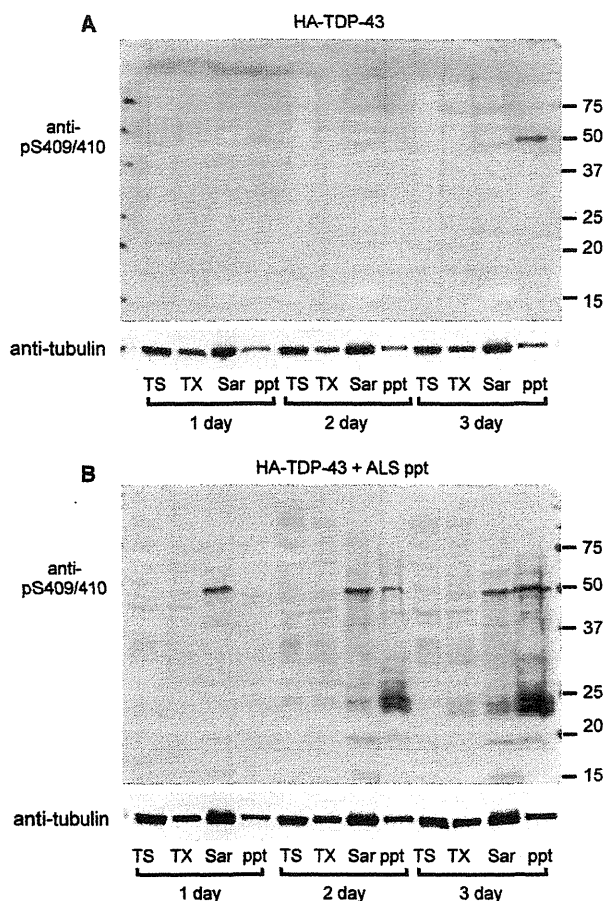


**Figure 2. Time Course of Production of TDP-43 CTFs**  
(A and B) Cells transiently expressing HA-TDP-43 plasmid treated without (A) or with (B) ALS ppt were incubated for 1–3 days and then harvested. Proteins were differentially extracted and subjected to immunoblot analyses. Blots were probed with anti-pS409/410.

plasmid and ALS ppt, surprisingly, full-length HA-TDP-43 was accumulated even on day 1, whereas CTFs were not detected in any fraction at this time (Figure 2B). On and after day 2, not only full-length HA-TDP-43 but also CTFs were aggregated in cells. Thus, intracellular aggregation of full-length TDP-43 precedes generation of TDP-43 CTFs, suggesting that production of CTFs is not essential for formation of intracellular TDP-43 aggregates.

#### Characteristic CTFs of Insoluble TDP-43 in Each Disease Type Were Reproduced in a Self-Templating Manner in Cultured Cells

TDP-43 proteinopathy is classified into four types based on the predominant TDP-43-positive structures: type A mainly includes FTL-D-TDP with GRN mutations, type B contains ALS and FTL-D-MND, type C is representative of sporadic FTL-D-TDP showing impairment of semantic memory, and type D refers to the pathology associated with inclusion body myopathy with early-onset

Paget's disease and frontotemporal dementia caused by VCP mutations (Mackenzie et al., 2011). Each type is also characterized biochemically by the patterns of insoluble TDP-43 CTFs detected with anti-pS409/410 (Hasegawa et al., 2008; Tsuji et al., 2012). We prepared Sar-ppt from several types of brains (Figure 3A) and introduced them as seeds into cells expressing a plasmid encoding TDP-43. After 3 days of incubation, cells were harvested and each Sar-ppt was analyzed by immunoblotting with anti-pS409/410. In Figures 3A and 3B, all seeds prepared from TDP-43 proteinopathy brains (Nos. 1–8), but not from DLB (No. 9) or Pick's disease (No. 10) brain, were shown to function as seeds for TDP-43 aggregation in cultured cells, but the seeding efficiencies were different: type A and B seeds were more effective than type C. No sample was available from FTL-D-TDP type D brain.

Next, to check whether each characteristic deposit of CTF was reproduced in cultured cells in the presence of each type of seed, we prepared insoluble fractions from TDP-43-expressing cells treated with seeds from each type of brain, and analyzed them by immunoblotting using anti-pS409/410. Interestingly, the band patterns of CTFs in the insoluble fraction (ppt) of cells expressing TDP-43 in the presence of each type of seed were different from each other, but quite similar to that of insoluble TDP-43 prepared as seeds from the corresponding patients (type A, B, or C), indicating that plasmid-derived TDP-43 is aggregated in a template-dependent manner in the presence of each type of seed (Figure 3C). These results suggest that seed-dependent TDP-43 aggregation, like prion aggregation, occurs in a self-templating manner. Insoluble TDP-43 from diseased brains appears to have features similar to those of pathogenic prion.

#### Insoluble TDP-43 Has Prion-like Properties

Next, we examined whether insoluble TDP-43 from brains of patients has prion-like characteristics. First, we tested whether detergent-insoluble TDP-43 prepared from cells containing TDP-43 aggregates as well as seeds from brains can promote intracellular TDP-43 aggregation. Triton X-100 (TX)-insoluble fraction was prepared as seeds from cells containing aggregates (Figure 4A, right panel) and introduced into cells. In a control experiment, we confirmed that insoluble seeds from cells expressing HA-TDP-43 treated with ALS ppt (HA-TDP-43+ALS ppt) did not serve efficiently as seeds for endogenous TDP-43 aggregation (Figure S3A). In cells expressing HA-TDP-43 and treated with TX-insoluble seeds from cells transfected with both HA-TDP-43 and ALS ppt, phosphorylated full-length HA-TDP-43 and CTFs were observed in the insoluble fraction (ppt; Figure 4A), whereas the band of phosphorylated full-length HA-TDP was hardly detectable in the insoluble fraction from cells expressing HA-TDP-43 and treated with TX-insoluble seed from cells without transfection (none) or treated with TX-insoluble seed from cells expressing HA-TDP-43 alone (HA-TDP-43). In immunocytochemical analyses of cells expressing HA-TDP-43 and treated with TX-insoluble seeds from cells transfected with both HA-TDP-43 and ALS ppt (HA-TDP-43+ALS ppt), we observed inclusions positive for both anti-pS409/410 and anti-Ub (Figure 4B), which were very similar to those observed in cells expressing

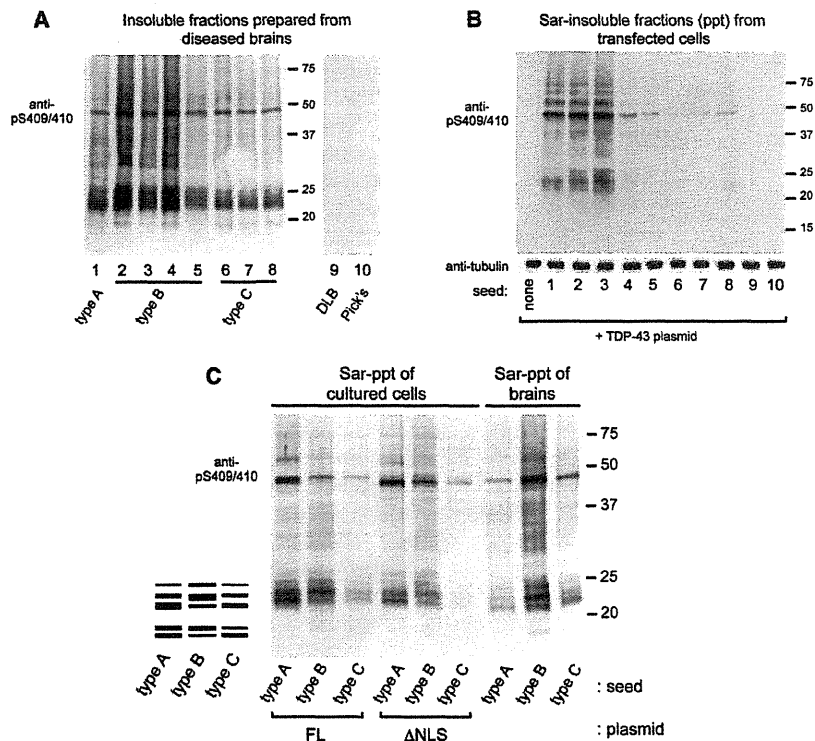


**Figure 3. Formation of Self-Templating Aggregates Induced by Insoluble TDP-43 from the Brains of Patients**

(A) Immunoblot analyses of Sar-ppt prepared from several diseased brains used as seeds. (B) Immunoblot analyses of Sar-ppt of cells expressing TDP-43 treated with each seed (Nos. 1–10). (C) Comparison of band patterns of Sar-ppt fractions from cells expressing full-length TDP-43 (FL) or TDP-43 lacking nuclear localization signal (78–84 residues:  $\Delta$ NLS) treated with type A, B, or C seed. Sar-ppt fractions from each of the diseased brains are shown next to cellular ppt fractions on the same blot. A schematic diagram of the band pattern of TDP-43 CTFs is also presented. Blots were probed using anti-pS409/410.

sary for seeding activity. Taken together, these results show that insoluble TDP-43 has prion-like properties, including repeated seeding ability and sensitivity to heat, proteinase, or formic acid.

#### Intracellular Aggregate Formation of TDP-43 Induces Cell Death in Cultured Cells

To examine whether intracellular TDP-43 aggregates cause neuronal dysfunction

leading to cell death, we measured the rate of cell death in cells containing intracellular TDP-43 aggregates by means of lactate dehydrogenase (LDH) assay. Cells transfected with TDP-43 were treated with insoluble fractions from TDP-43 proteinopathy brains or Pick's disease brain and incubated for 3 days, followed by LDH assay. As shown in Figure 5A, the rate of cell death was almost 5% in cells treated only with insoluble fractions from type B or plasmid transfection, whereas it was ~20% in cells expressing TDP-43 and treated with each TDP-43 proteinopathy brain extract. These cell lysates were also analyzed by immunoblotting. Increased cell death of these cells was accompanied by deposition of phosphorylated TDP-43 in the Sar-ppt fraction (Figure 5B). However, no significant cell death was observed in cells expressing TDP-43 and treated with Pick's disease brain extract, in which phosphorylated TDP-43 was not deposited. These results suggest that increased cell death of cells containing TDP-43 aggregates is correlated with the amount of intracellular TDP-43 aggregates.

HA-TDP-43 treated with ALS ppt (Figure 1E). These results indicate that TX-insoluble seeds produced from cells containing TDP-43 aggregates can function as seeds for further aggregation of TDP-43. We also checked the effects of heat treatment or proteinase digestion of insoluble TDP-43 on seeding ability. Each type of seed was treated or not treated at 100°C for 5 min (boiling) and analyzed by immunoblotting with anti-pS409/410. No marked differences in the band patterns of each type of seed were seen before or after the boiling treatment (Figure 4C, left panel). Then, these seeds were introduced into TDP-43-expressing cells, and Sar-ppts prepared from the cells were analyzed by immunoblotting with anti-pS409/410 (Figures 4C and S3B). In the case of type A seed, the seeding effect on TDP-43 aggregation was unaffected by boiling, whereas the ability of type B and C seeds to induce TDP-43 aggregation was almost abrogated after boiling (Figure 4C, middle and right panels). All of these seeds were easily degraded into <20 kDa CTFs by Proteinase K (ProK) treatment (Figure 4D, left panel). However, seeding ability to induce intracellular TDP-43 aggregation was retained even after ProK digestion (Figure 4D, middle and right panels, and Figure S3C).

Furthermore, we tested whether formic acid, which destroys the  $\beta$ -sheet structure of proteins, influences the seeding ability of insoluble TDP-43. As shown in Figures 4E, S3D, and S3E, insoluble fractions from type A, B, and C brains treated with formic acid did not induce intracellular TDP-43 aggregation, suggesting that  $\beta$ -sheet-rich structure is neces-

leading to cell death, we measured the rate of cell death in cells containing intracellular TDP-43 aggregates by means of lactate dehydrogenase (LDH) assay. Cells transfected with TDP-43 were treated with insoluble fractions from TDP-43 proteinopathy brains or Pick's disease brain and incubated for 3 days, followed by LDH assay. As shown in Figure 5A, the rate of cell death was almost 5% in cells treated only with insoluble fractions from type B or plasmid transfection, whereas it was ~20% in cells expressing TDP-43 and treated with each TDP-43 proteinopathy brain extract. These cell lysates were also analyzed by immunoblotting. Increased cell death of these cells was accompanied by deposition of phosphorylated TDP-43 in the Sar-ppt fraction (Figure 5B). However, no significant cell death was observed in cells expressing TDP-43 and treated with Pick's disease brain extract, in which phosphorylated TDP-43 was not deposited. These results suggest that increased cell death of cells containing TDP-43 aggregates is correlated with the amount of intracellular TDP-43 aggregates.

#### Intracellular Accumulation of TDP-43 Aggregates Elicits Proteasome Dysfunction

Previously, we reported that proteasome activity was suppressed in cells containing intracellular  $\alpha$ -synuclein aggregates (Nonaka et al., 2010). To examine whether intracellular aggregates of TDP-43 also induce proteasome dysfunction, we assayed proteasome activity in cells containing TDP-43 aggregates by using the GFP-CL1 reporter (Bence et al., 2001), which is available to monitor proteasome activity in cultured cells (Nonaka and Hasegawa, 2009; Nonaka et al., 2010).

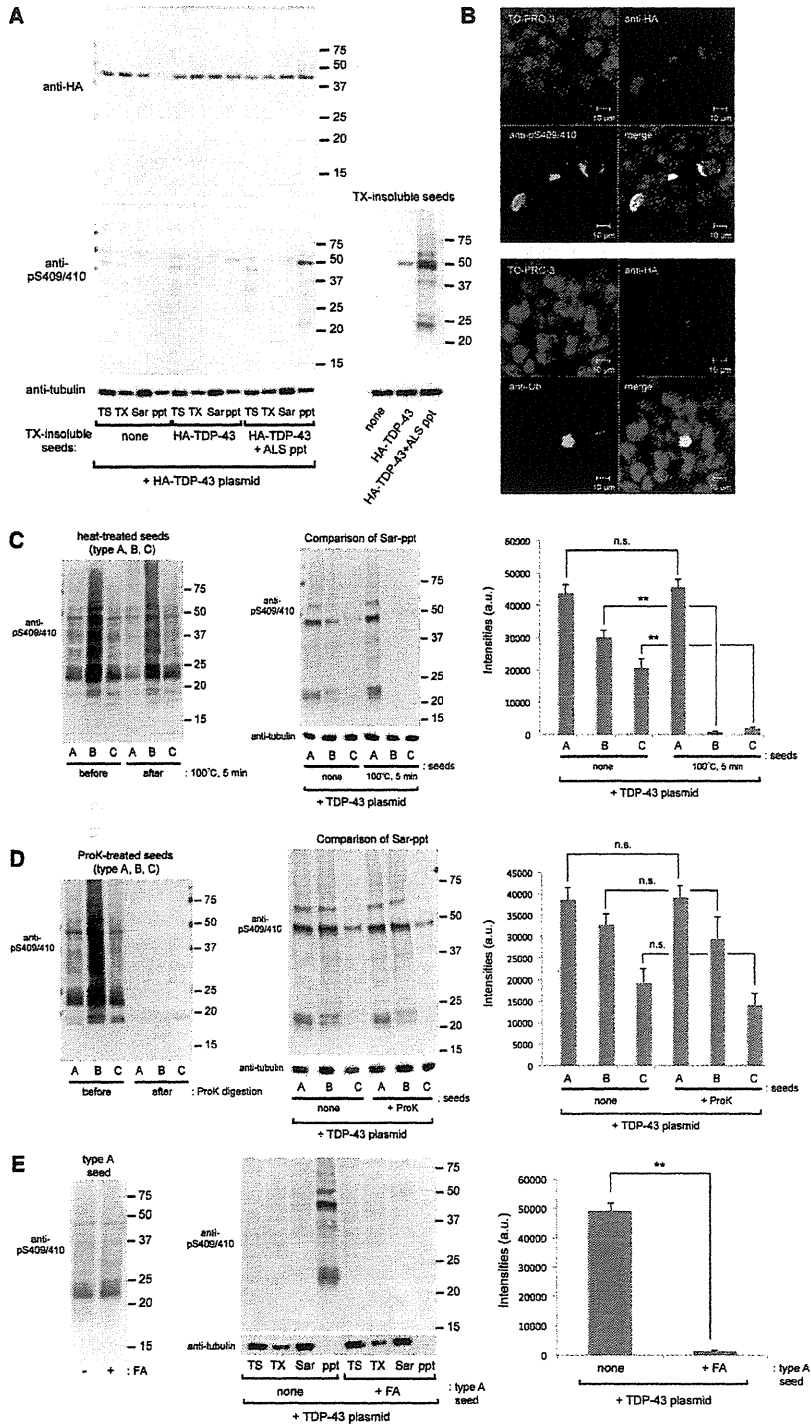


**Figure 4. Characterization of the Prion-like Properties of Detergent-Insoluble TDP-43 from Brains**

(A) Immunoblot analyses of cells expressing HA-TDP-43 and treated with Triton X-100-insoluble fractions (TX-insoluble seeds) prepared from the following cells, using anti-HA (upper) and anti-pS409/410 (lower): none, mock cells; HA-TDP-43, cells expressing HA-TDP-43; and HA-TDP-43+ALS ppt, cells expressing HA-TDP-43 and treated with ALS ppt. These TX-insoluble seeds (10 µg each) were also immunoblotted with anti-pS409/410 (lower right).

(B) Confocal laser microscopy analyses of cells expressing HA-TDP-43 and treated with TX-insoluble seed from cells transfected with both HA-TDP-43 and ALS ppt (HA-TDP-43+ALS ppt) immunostained with anti-HA (red), anti-pS409/410 (green), or anti-Ub (green), and counterstained with TO-PRO-3 (blue). Scale bars: 10 µm.

(C) Effect of heat treatment on the seeding ability of each type of seed. Each seed before and after heat treatment (100°C for 5 min) was analyzed by immunoblotting using anti-pS409/410 (left). Then, cells expressing TDP-43 were treated with these fractions as seeds. After 3 days of incubation, Sar-ppt fractions were prepared and analyzed by immunoblotting using anti-pS409/410 (middle). The immunoreactivity of each lane that was positive for anti-pS409/410 was quantified and the results are expressed as means + SEM (n = 3). \*\*p < 0.0001 by Student's t test; n.s., not significant; a.u., arbitrary unit. See also Figure S3.

(D) Effect of ProK on the seeding ability of each type of seed. Each seed before and after ProK digestion (final 20 µg/mL ProK at 37°C for 30 min) was analyzed by immunoblotting using anti-pS409/410 (left). Then, cells expressing TDP-43 were treated with these fractions as seeds. After 3 days of incubation, the Sar-ppt fractions were analyzed by immunoblotting using anti-pS409/410 (middle). The immunoreactivity of each lane that was positive for anti-pS409/410 was quantified and the results are expressed as means + SEM (n = 3). n.s., not significant; a.u., arbitrary unit. See also Figure S3.

(E) Effect of formic acid (FA) on the seeding ability of type A seed. Type A seed with or without FA treatment was analyzed by immunoblotting using anti-pS409/410 (left). Then, cells expressing TDP-43 were treated with these fractions as seeds. After 3 days of incubation, fractionated samples were analyzed by immunoblotting using anti-pS409/410 (right). The immunoreactivity of ppt fractions that were positive for anti-pS409/410 was quantified and the results are expressed as means + SEM (n = 3). \*\*p < 0.0001 by Student's t test. a.u., arbitrary unit. See also Figure S3.

Cells were transfected with TDP-43 and GFP-CL1 plasmids overnight, followed by transduction of ALS ppt. After 3 days of incubation, the cells were analyzed by confocal microscopy and immunoblotting. As shown in Figures 6A and 6B,

GFP fluorescence in cells transfected with GFP-CL1 alone was very low due to degradation of GFP-CL1 by proteasome. When cells expressing GFP-CL1 were treated with proteasome inhibitor MG132 (0.1 µM), GFP fluorescence intensity

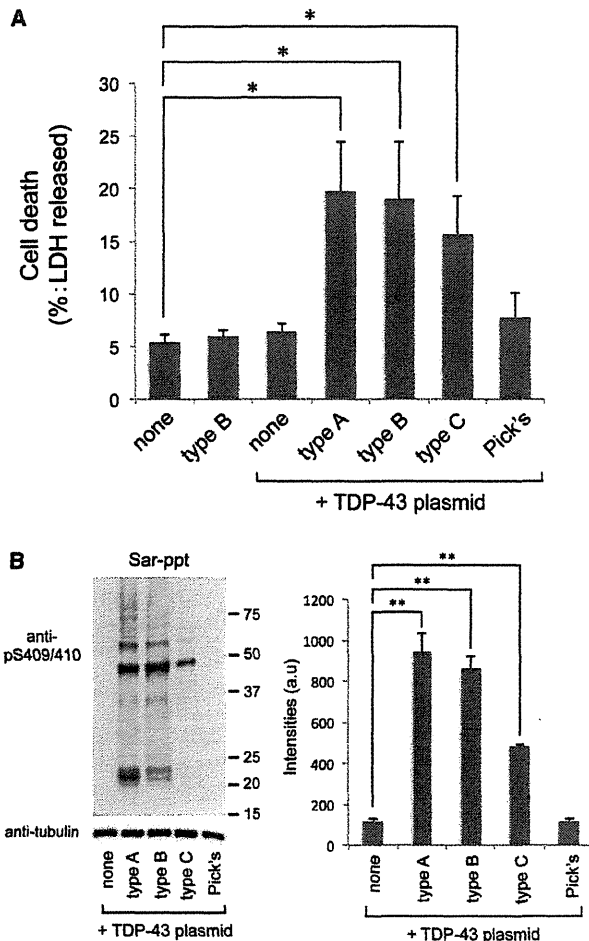


**Figure 5. Cell Death Induced by the Formation of Intracellular TDP-43 Aggregates**

(A) The extent of cell death of transfected cells was quantified by an LDH release assay. Cells treated with type B seed alone (type B), cells transfected with TDP-43 plasmid alone, or cells expressing TDP-43 and treated with Sar-ppt from type A, B, or C, or Pick's disease brains were cultured, and a cell death assay was performed 3 days thereafter. The results are expressed as means  $\pm$  SEM ( $n = 5$ ). \* $p < 0.05$  versus "none" by Student's *t* test.

(B) Immunoblot analyses of Sar-ppt from cells expressing TDP-43 and treated with extracts of type A, B, C, and Pick's disease brains, using anti-pS409/410. Immunoreactivity to anti-pS409/410 was quantified in each lane. The results are expressed as means  $\pm$  SEM ( $n = 3$ ). \*\* $p < 0.001$  versus "none" by Student's *t* test. a.u., arbitrary unit.

was significantly higher. GFP fluorescence in cells transfected with TDP-43 alone or treated with ALS ppt alone was as low as that in cells expressing only GFP-CL1, whereas it was significantly higher in cells expressing TDP-43 and treated with ALS ppt. We confirmed that cells containing phosphorylated TDP-43 aggregates were strongly positive for GFP (Figure 6C). These results suggest that proteasome activity is suppressed in cells harboring intracellular TDP-43 aggregates.

### Phosphorylated TDP-43 Aggregates Are Propagated between Cultured Cells

To examine whether TDP-43 aggregates can be transferred between cultured cells, we performed coculture experiments. SH-SY5Y cells expressing only DsRed were cocultured with SH-SY5Y cells harboring phosphorylated TDP-43 aggregates in a 1:1 ratio. After incubation for 3 days, the cells were stained with anti-pS409/410 and analyzed by confocal laser microscopy. The presence of phosphorylated TDP-43 aggregates immunolabeled with Alexa-488 in cells expressing DsRed would indicate that phosphorylated TDP-43 aggregates could spread to cells that originally did not contain these aggregates. As shown in Figures 7A and 7B, phosphorylated TDP-43 aggregates (green) were found in the cytoplasm of cells expressing DsRed. The percentage of DsRed-positive cells that also contained phosphorylated TDP-43 aggregates was calculated to be  $2.9\% \pm 0.8\%$ . In three-dimensional image modeling of a DsRed-expressing cell with TDP-43 aggregates, the signal of phosphorylated TDP-43 aggregates was merged with that of DsRed in the X-Z and Y-Z cross-sections (Figure 7B).

Next, we examined how TDP-43 aggregates are released from cells. It has been hypothesized that protein aggregates are released via exosome (Fevrier et al., 2004; Goedert et al., 2010). To investigate whether this mechanism operates for TDP-43 aggregates, we prepared exosome fractions from cells expressing TDP-43 plasmid alone, cells treated with ALS ppt alone, or cells expressing TDP-43 and treated with ALS ppt using the ExoQuick-TC kit (SBI). Immunoblot analyses showed that in cells expressing TDP-43 and treated with ALS ppt, the band intensity of full-length TDP-43 in the exosome fraction was significantly increased as compared with that in cells transfected with TDP-43 plasmid or ALS ppt alone (Figure 7C), whereas expression of the exosome marker protein CD63 was similar in all of the exosome fractions. These results suggest the possibility that exosome may contribute to the release of intracellular TDP-43 aggregates.

### DISCUSSION

Prion-like propagation of aggregated proteins in neurodegenerative diseases is well established (Clavaguera et al., 2009; Desplats et al., 2009; Frost et al., 2009; Goedert et al., 2010; Kordower et al., 2008; Li et al., 2008; Luk et al., 2009; Nonaka et al., 2010; Masuda-Suzukake et al., 2013; Polymenidou and Cleveland, 2011; Ren et al., 2009). Here, we show that insoluble TDP-43 prepared from TDP-43 proteinopathy brains (type A, B, and C) can function as seeds for intracellular TDP-43 aggregation in cultured cells. Type A, B, and C brains showed distinct banding patterns of TDP-43 CTFs in immunoblot analyses with anti-pS409/410 (Hasegawa et al., 2008; Tsuji et al., 2012). The band patterns of characteristic CTFs are thought to reflect structural differences of TDP-43 fibrils deposited in each type of brain (Hasegawa et al., 2008; Tsuji et al., 2012). Interestingly, band patterns of CTFs characteristic of the individual seeds were seen in intracellular TDP-43 aggregates in cultured cells, indicating that plasmid-derived TDP-43 aggregation occurs in a self-templating manner. The seeding activity of insoluble TDP-43 from patients' brains was stable against detergents, heat



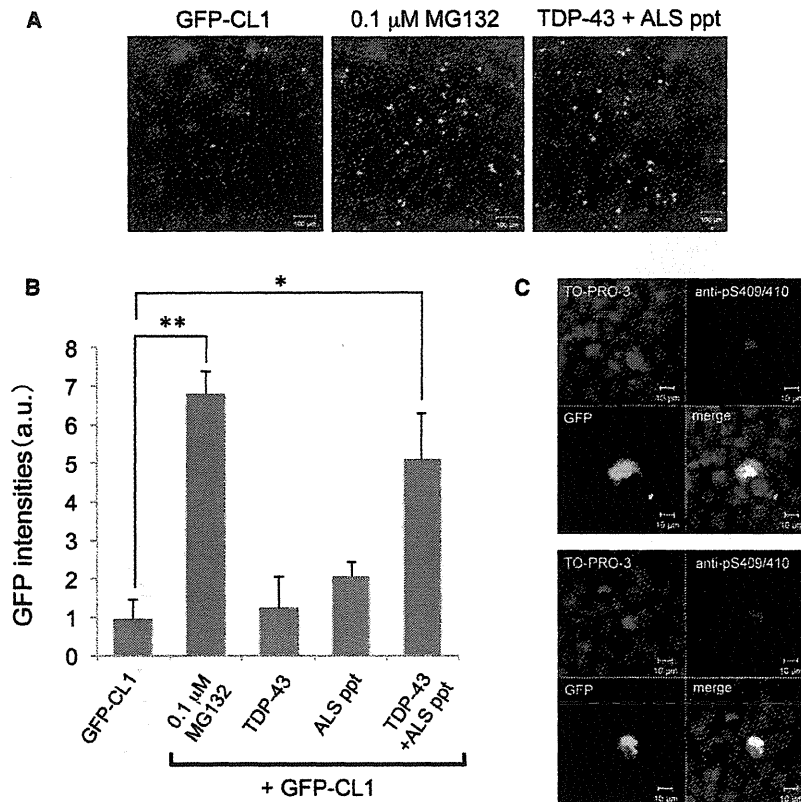


**Figure 6. Proteasome Dysfunction in Cells Bearing Intracellular TDP-43 Aggregates** (A–C) SH-SY5Y cells transfected with both GFP-CL1 and TDP-43 were treated with ALS ppt for 2 days.

(A) As a control, cells expressing GFP-CL1 with or without 0.1  $\mu$ M MG132 or ALS ppt, and cells expressing both GFP-CL1 and TDP-43 were also analyzed.

(B) The intensity of GFP fluorescence in these cells was quantified. The results are expressed as means  $\pm$  SEM (n = 3). \*p < 0.05; \*\*p < 0.001 versus the value of GFP-CL1 by Student's t test. a.u., arbitrary unit.

(C) Cells transfected with both GFP-CL1 and TDP-43 and treated with ALS ppt were stained with anti-pS409/410.

treatment, or proteolytic digestion, and cell-to-cell transmission ability was retained. Formic acid abrogated the seeding ability, suggesting that  $\beta$ -sheet structure in insoluble TDP-43 is indispensable for this ability. Thus, insoluble TDP-43 in the brains of patients has the characteristics of a pathogenic prion, suggesting that TDP-43 proteinopathy involves mechanisms similar to those of prion disease. It remains unclear, however, how protein aggregates spread between cells in vivo. It seems likely that prion-like aggregates are released from cells and taken up by neighboring cells, where they penetrate the cytoplasm and act as nuclei for further aggregation (Goedert et al., 2010). Prions are transferred between cultured cells via exosomes or tunneling nanotubes (Fevrier et al., 2004; Gousset et al., 2009), and our results indicate that TDP-43 aggregates may also be transferred from cell to cell at least partly via exosomes. Further investigation is needed to elucidate in detail the mechanisms of intercellular propagation of protein aggregates in vitro and in vivo. Nevertheless, taken together, our data suggest that TDP-43 proteinopathy can be classified as a prion disease.

Phosphorylated TDP-43 CTFs, as well as phosphorylated full-length TDP-43, are deposited in affected neurons in TDP-43 proteinopathy (Hasegawa et al., 2008, 2011). TDP-43 CTFs identified in FTLD-TDP brains are more prone to form aggregates than the full-length molecule in cultured cells (Igaz et al., 2009; Nonaka et al., 2009). Further, they bind with full-length TDP-43 and may facilitate aggregation of full-length TDP-43 in cultured cells (Budini et al., 2012; Nonaka et al., 2009; Zhang et al.,

2009). Therefore, generation of pathogenic TDP-43 CTFs may be crucial for the formation of intracellular TDP-43 inclusions leading to neuronal cell death. However, our time-course immunoblotting analyses (Figure 2) showed that full-length TDP-43 aggregation preceded the deposition of CTFs, suggesting that cleavage of TDP-43 to produce CTFs is not a trigger for intracellular TDP-43 aggregate formation. Thus, it appears that the generation of CTFs is a consequence of degradation of phosphorylated

full-length TDP-43 to eliminate abnormal and toxic aggregates of TDP-43, rather than a cause of aggregation of full-length TDP-43. In other words, TDP-43 CTFs deposited in affected neurons represent the residual stable core portion of TDP-43 aggregates left after degradation by intracellular proteolytic systems. Abnormal posttranslational modifications and abnormal structure of seeds for aggregation are important for reproducing the pathological and biochemical features of TDP-43 inclusions found in the brains of patients with TDP-43 proteinopathy in cultured cells. Indeed, intracellular TDP-43 aggregates obtained using recombinant TDP-43 fibrils as seeds appeared as very small dot-like structures without phosphorylation (Furukawa et al., 2011), and were quite different from the TDP-43 inclusions found in the brains of patients. Our model for seeded aggregation of TDP-43 seems consistent with the pathological and biochemical changes found in the brains of patients with TDP-43 proteinopathy: in the model, aggregated TDP-43 is phosphorylated and ubiquitinated, and immunoreactivity of TDP-43 in nuclei of cells containing cytoplasmic TDP-43 aggregates is relatively weak. We also observed significant cell death and proteasome dysfunction associated with the presence of intracellular TDP-43 aggregates. It is possible that such proteasome dysfunction is caused by overloading of the ubiquitin-proteasome system with ubiquitinated proteins, including TDP-43 aggregates. The resulting suppression of proteasome activity might induce cell death. We previously observed a similar phenomenon (Nonaka et al., 2010); i.e., seed-dependent intracellular

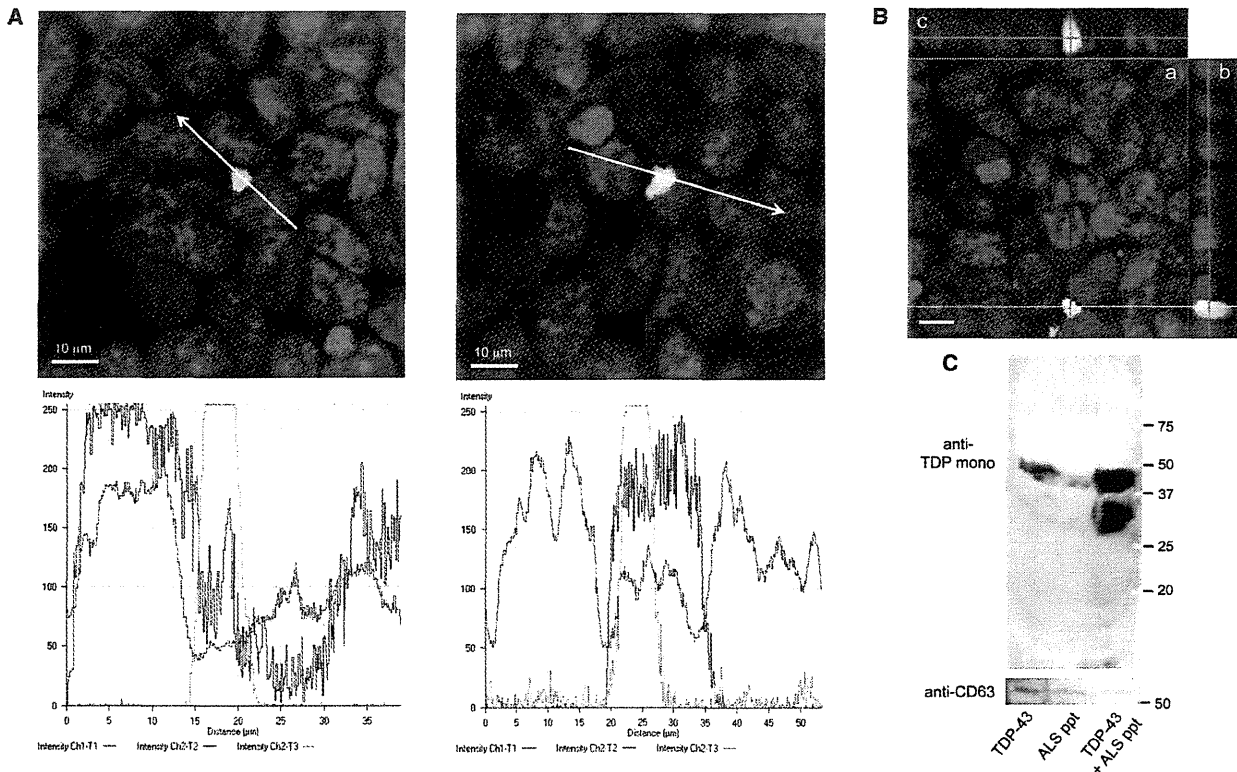


**Figure 7. Intracellular TDP-43 Aggregates Are Released in Association with Exosome**

(A) Coculture of cells expressing DsRed and cells having intracellular TDP-43 aggregates in a 1:1 ratio. After incubation for 3 days, cells were stained with pS409/410 (green) and counterstained with TO-PRO-3 (blue). The graphs show the intensity distribution profile of DsRed (red line), phosphorylated TDP-43 (green line), and TO-PRO-3, a nuclear marker (blue line), in the merged image. Scale bars: 10  $\mu$ m.

(B) Cross-sections of reconstructed TDP-43 aggregates in these cocultured cells. (a) One of the optical sections (X-Y) at the depth indicated with blue lines in (b) and (c). (b) Cross-sectional Y-Z image along the green line indicated in (a). (c) Cross-sectional X-Z image along the red line indicated in (a). Red, DsRed; green, phosphorylated TDP-43 aggregate positive for anti-pS409/410; blue, TO-PRO-3 (nuclei). Scale bars: 10  $\mu$ m.

(C) Immunoblot analyses of exosome fractions prepared from culture medium of cells expressing TDP-43 (TDP-43), cells treated with ALS ppt alone (ALS ppt), and cells expressing TDP-43 and treated with ALS ppt (TDP-43+ALS ppt). Blots were probed with anti-TDP-43 monoclonal (ProteinTech) and an antibody against CD63 (SBI).

aggregation of  $\alpha$ -synuclein caused proteasome dysfunction and cell death.

In summary, our results show that insoluble TDP-43 in the brains of patients has prion-like features, and we consider that the onset and progression of TDP-43 proteinopathy may be associated with the propagation of TDP-43 aggregates between neuronal cells. If this is so, suppressing the propagation of aggregated proteins may be a new therapeutic strategy for many neurodegenerative diseases.

## EXPERIMENTAL PROCEDURES

### Preparation of Detergent-Insoluble Fractions from Brains of Patients

Human brain tissues were obtained from Fukushima Hospital, Aichi Medical University (Aichi, Japan), Shizuoka Institute of Epilepsy and Neurological Disorders (Shizuoka, Japan), and Tokyo Metropolitan Institute of Gerontology (Tokyo, Japan). This study was approved by the local research ethics committee of Tokyo Metropolitan Institute of Medical Science (approval No. 12-3). The subjects included four patients with ALS, one with FTLD-TDP

type A, three with FTLD-TDP type C, one with dementia with Lewy bodies, and one with Pick's disease. All patients with ALS met the revised El Escorial criteria for ALS (Brooks, 1994) without dementia. All patients with FTLD-TDP met the clinical diagnostic criteria of FTLD (Neary et al., 1998), and TDP-43 subtypes were classified according to published guidelines (Mackenzie et al., 2011).

Brain samples (0.5 g) from patients with ALS, FTLD-TDP, or Pick's disease were each homogenized in 2.5 ml of homogenization buffer (HB: 10 mM Tris-HCl, pH 7.5 containing 0.8 M NaCl, 1 mM EGTA, 1 mM dithiothreitol). Sarkosyl was added to the lysates (final concentration: 1%), which were then incubated for 30 min at 37°C, and centrifuged at 12,000 g for 10 min at room temperature. The supernatant was further centrifuged at 100,000 g for 10 min at room temperature. The pellet was suspended in 2 ml PBS by sonication. Lysates were divided into four tubes (each 500  $\mu$ L) and centrifuged at 100,000 g for 20 min at room temperature. The resulting pellets were used as the detergent-insoluble fraction (ppt).

For immuno-electron microscopy analyses, the detergent-insoluble fractions prepared from brains were placed on collodion-coated, 300-mesh copper grids and stained with anti-pS409/410 and 2% (v/v) phosphotungstate. Micrographs were recorded on a JEOL JEM-1400 electron microscope.

In ID experiments, mixtures of anti-pS409/410 and anti-TDP-43 polyclonal antibody (Proteintech; 2  $\mu$ l each) were added to 20  $\mu$ l of ALS ppt suspension

in PBS, followed by addition of 10  $\mu$ l of protein G-Sepharose (Sigma). After overnight incubation at 4°C, the supernatant was recovered. As a control, the other half of the lysate was incubated with a mixture of nonspecific mouse and rabbit immunoglobulin G (IgG; Cosmo Bio) and the same amount of protein G-Sepharose. An 8  $\mu$ l aliquot of the supernatant was introduced into cells as described below.

In formic acid treatment, the detergent-insoluble fractions were suspended in 100  $\mu$ l of 100% (v/v) formic acid (Nacalai Tesque) and incubated at room temperature for 30 min. After incubation, 900  $\mu$ l of water was added and the mixtures were evaporated. The resulting residues were suspended in 500  $\mu$ l of 0.1 M triethylammonium bicarbonate buffer (Fluka) and evaporated again. The residues were also suspended in 500  $\mu$ l of water and centrifuged at 100,000 g for 20 min at room temperature. The resulting pellets were suspended in 100  $\mu$ l of PBS and the mixtures were used for introduction experiments (see below).

#### Cell Culture and Transfection of Expression Plasmids

Human neuroblastoma SH-SY5Y cells obtained from ATCC were cultured in Dulbecco's modified Eagle's medium (DMEM)/F12 medium (Sigma-Aldrich) supplemented with 10% (v/v) fetal calf serum, penicillin-streptomycin-glutamine (Gibco), and MEM nonessential amino acids solution (Gibco). The cells were maintained at 37°C under a humidified atmosphere of 5% (v/v) CO<sub>2</sub> in air. They were grown to 50% confluence in six-well culture dishes for transient expression and then transfected with expression plasmids (usually 1  $\mu$ g) using FuGENE6 (Roche) according to the manufacturer's instructions. Under our conditions, the efficiency of transfection using pEGFP-C1 vector was 20%–30%.

#### Introduction of Insoluble Proteins into Cells

Detergent-insoluble fractions prepared as described above were suspended in 150  $\mu$ l PBS by sonication. Then 5  $\mu$ g of insoluble fraction was mixed with 120  $\mu$ l of Opti-MEM (Gibco), and 62.5  $\mu$ l of Multifectam was added. After incubation for 30 min at room temperature, 62.5  $\mu$ l of Opti-MEM was added and incubation was continued for 5 min at room temperature. Then, the mixtures were added to cells (mock cells or cells expressing HA-TDP-43, non-tagged TDP-43, or TDP-43  $\Delta$ NLS) and incubation was continued for 6 hr in a CO<sub>2</sub> incubator. After incubation, the medium was changed to fresh DMEM/F12 and culture was continued for the indicated period in each case. The cells were harvested and cellular proteins were differentially extracted and immunoblotted with the indicated antibodies, as previously described (Nonaka et al., 2010). Under our conditions, the efficiency of introduction of brain extracts was ~10%.

#### Confocal Microscopy

SH-SY5Y cells on coverslips were transfected with the indicated plasmids and cultured for 14 hr as described above. Then, the detergent-insoluble fraction was introduced and culture was continued for ~1–2 days. After fixation with 4% paraformaldehyde, cells were stained with the appropriate primary and secondary antibodies as described previously (Nonaka et al., 2010). Fluorescence was analyzed with a laser scanning confocal fluorescence microscope (LSM5 Pascal; Carl Zeiss). Confocal Z slices with an interval of 0.2 or 0.5  $\mu$ m were obtained and reconstructed for three-dimensional observation using LSM5 Pascal v 4.0 software.

#### Cell Death Assay

Cell death assays were performed using a CytoTox 96 Non-Radioactive Cytotoxicity Assay Kit (Promega).

#### Assay of Proteasome Activity

In a GFP-reporter assay to monitor proteasome activity in cultured cells by confocal laser microscopy, SH-SY5Y cells that had been transfected with pcDNA3-HA-TDP-43 (1  $\mu$ g) and GFP-CL1 (0.3  $\mu$ g) using FuGENE6 and then treated with detergent-insoluble fraction of ALS brain were grown on coverslips for 2 days or treated with 0.1  $\mu$ M MG132 overnight (Nonaka and Hasegawa, 2009; Nonaka et al., 2010). These cells were analyzed with the use of a laser-scanning confocal fluorescence microscope (LSM5Pascal; Carl Zeiss).

#### Coculture of Cells

SH-SY5Y cells transiently expressing DsRed (3 days after transfection) were mixed equally with cells expressing TDP-43 and treated with ALS ppt (3 days after introduction of ALS ppt). The cocultured cells were grown for a further 3 days, fixed with 4% paraformaldehyde, stained with anti-pS409/410 and TO-PRO-3, and observed under a laser-scanning confocal fluorescence microscope (LSM5Pascal; Carl Zeiss).

#### Preparation of Exosome Fractions

Exosome fractions were prepared from 4 ml of culture medium of cells expressing TDP-43, cells treated with ALS ppt, or cells transfected with both TDP-43 and ALS ppt, which had been cultured for 3 days after transfection, using an ExoQuick-TC kit from SBI according to the manufacturer's protocol. The exosome fractions were dissolved in 100  $\mu$ l of SDS sample buffer and immunoblotted.

#### Statistical Analysis

Statistical analyses were performed using GraphPad Prism 4 software (GraphPad Software). Biochemical data were statistically analyzed using the unpaired, two-tailed Student's t test. A p value of  $\leq 0.05$  was considered to be statistically significant. For further details regarding the materials and methods used in this work, see Extended Experimental Procedures.

#### SUPPLEMENTAL INFORMATION

Supplemental Information includes Extended Experimental Procedures and three figures and can be found with this article online at <http://dx.doi.org/10.1016/j.celrep.2013.06.007>.

#### ACKNOWLEDGMENTS

We thank Makiko Yamashita and Masato Hosokawa for helpful comments. This work was supported by a Grant-in-Aid for Scientific Research (C) (JSPS KAKENHI 22500345 to T.N.), a Grant-in-Aid for Scientific Research (S) (JSPS KAKENHI 23228004 to M.H.) a Grant-in-Aid for Scientific Research (A) (JSPS KAKENHI 23240050 to M.H.), MHLW Grant (Number 12946221 to M.H.), a Grant-in-Aid for Scientific Research on Innovative Area "Brain Environment" (MEXT KAKENHI 24111556 to T.N.), and a grant from the Takeda Science Foundation (to T.N.).

Received: March 12, 2013

Revised: May 17, 2013

Accepted: June 6, 2013

Published: July 3, 2013

#### REFERENCES

- Arai, T., Hasegawa, M., Akiyama, H., Ikeda, K., Nonaka, T., Mori, H., Mann, D., Tsuchiya, K., Yoshida, M., Hashizume, Y., and Oda, T. (2006). TDP-43 is a component of ubiquitin-positive tau-negative inclusions in frontotemporal lobar degeneration and amyotrophic lateral sclerosis. *Biochem. Biophys. Res. Commun.* 351, 602–611.
- Arai, T., Hasegawa, M., Nonaka, T., Kametani, F., Yamashita, M., Hosokawa, M., Niizato, K., Tsuchiya, K., Kobayashi, Z., Ikeda, K., et al. (2010). Phosphorylated and cleaved TDP-43 in ALS, FTL and other neurodegenerative disorders and in cellular models of TDP-43 proteinopathy. *Neuropathology* 30, 170–181.
- Bence, N.F., Sampat, R.M., and Kopito, R.R. (2001). Impairment of the ubiquitin-proteasome system by protein aggregation. *Science* 292, 1552–1555.
- Bigio, E.H., Wu, J.Y., Deng, H.X., Bit-Ivan, E.N., Mao, Q., Ganti, R., Peterson, M., Siddique, N., Geula, C., Siddique, T., and Mesulam, M. (2013). Inclusions in frontotemporal lobar degeneration with TDP-43 proteinopathy (FTLD-TDP) and amyotrophic lateral sclerosis (ALS), but not FTL with FUS proteinopathy (FTLD-FUS), have properties of amyloid. *Acta Neuropathol.* 125, 463–465.
- Braak, H., and Braak, E. (1991). Neuropathological staging of Alzheimer-related changes. *Acta Neuropathol.* 82, 239–259.

- Braak, H., Del Tredici, K., Rüb, U., de Vos, R.A., Jansen Steur, E.N., and Braak, E. (2003). Staging of brain pathology related to sporadic Parkinson's disease. *Neurobiol. Aging* 24, 197–211.
- Brooks, B.R. (1994). El Escorial World Federation of Neurology criteria for the diagnosis of amyotrophic lateral sclerosis. Subcommittee on Motor Neuron Diseases/Amyotrophic Lateral Sclerosis of the World Federation of Neurology Research Group on Neuromuscular Diseases and the El Escorial "Clinical Limits of Amyotrophic Lateral Sclerosis" workshop contributors. *J. Neurol. Sci.* 124(Suppl), 96–107.
- Budini, M., Buratti, E., Stuani, C., Guarnaccia, C., Romano, V., De Conti, L., and Baralle, F.E. (2012). Cellular model of TAR DNA binding protein 43 (TDP-43) aggregation based on its C-terminal Q/N rich region. *J. Biol. Chem.* 287, 7512–7525.
- Buratti, E., and Baralle, F.E. (2009). The molecular links between TDP-43 dysfunction and neurodegeneration. *Adv. Genet.* 66, 1–34.
- Buratti, E., Dörk, T., Zuccato, E., Pagani, F., Romano, M., and Baralle, F.E. (2001). Nuclear factor TDP-43 and SR proteins promote in vitro and in vivo CFTR exon 9 skipping. *EMBO J.* 20, 1774–1784.
- Clavaguera, F., Bolmont, T., Crowther, R.A., Abramowski, D., Frank, S., Probst, A., Fraser, G., Stalder, A.K., Beibel, M., Staufenbiel, M., et al. (2009). Transmission and spreading of tauopathy in transgenic mouse brain. *Nat. Cell Biol.* 11, 909–913.
- de Calignon, A., Polydoro, M., Suárez-Calvet, M., William, C., Adamowicz, D.H., Kopelkina, K.J., Pittstick, R., Sahara, N., Ashe, K.H., Carlson, G.A., et al. (2012). Propagation of tau pathology in a model of early Alzheimer's disease. *Neuron* 73, 685–697.
- Desplats, P., Lee, H.J., Bae, E.J., Patrick, C., Rockenstein, E., Crews, L., Spencer, B., Masliah, E., and Lee, S.J. (2009). Inclusion formation and neuronal cell death through neuron-to-neuron transmission of alpha-synuclein. *Proc. Natl. Acad. Sci. USA* 106, 13010–13015.
- Fevrier, B., Vilette, D., Archer, F., Loew, D., Faigle, W., Vidal, M., Laude, H., and Raposo, G. (2004). Cells release prions in association with exosomes. *Proc. Natl. Acad. Sci. USA* 101, 9683–9688.
- Frost, B., Jacks, R.L., and Diamond, M.I. (2009). Propagation of tau misfolding from the outside to the inside of a cell. *J. Biol. Chem.* 284, 12845–12852.
- Furukawa, Y., Kaneko, K., Watanabe, S., Yamanaka, K., and Nukina, N. (2011). A seeding reaction recapitulates intracellular formation of Sarkosyl-insoluble transactivation response element (TAR) DNA-binding protein-43 inclusions. *J. Biol. Chem.* 286, 18664–18672.
- Goedert, M., Clavaguera, F., and Tolnay, M. (2010). The propagation of prion-like protein inclusions in neurodegenerative diseases. *Trends Neurosci.* 33, 317–325.
- Gousset, K., Schiff, E., Langevin, C., Marjanovic, Z., Caputo, A., Browman, D.T., Chenouard, N., de Chaumont, F., Martino, A., Enninga, J., et al. (2009). Prions hijack tunnelling nanotubes for intercellular spread. *Nat. Cell Biol.* 11, 328–336.
- Guo, W., Chen, Y., Zhou, X., Kar, A., Ray, P., Chen, X., Rao, E.J., Yang, M., Ye, H., Zhu, L., et al. (2011). An ALS-associated mutation affecting TDP-43 enhances protein aggregation, fibril formation and neurotoxicity. *Nat. Struct. Mol. Biol.* 18, 822–830.
- Hasegawa, M., Arai, T., Nonaka, T., Kametani, F., Yoshida, M., Hashizume, Y., Beach, T.G., Buratti, E., Baralle, F., Morita, M., et al. (2008). Phosphorylated TDP-43 in frontotemporal lobar degeneration and amyotrophic lateral sclerosis. *Ann. Neurol.* 64, 60–70.
- Hasegawa, M., Nonaka, T., Tsuji, H., Tamaoka, A., Yamashita, M., Kametani, F., Yoshida, M., Arai, T., and Akiyama, H. (2011). Molecular dissection of TDP-43 proteinopathies. *J. Mol. Neurosci.* 45, 480–485.
- Igaz, L.M., Kwong, L.K., Chen-Plotkin, A., Winton, M.J., Unger, T.L., Xu, Y., Neumann, M., Trojanowski, J.Q., and Lee, V.M. (2009). Expression of TDP-43 C-terminal fragments in vitro recapitulates pathological features of TDP-43 proteinopathies. *J. Biol. Chem.* 284, 8516–8524.
- Kordower, J.H., Chu, Y., Hauser, R.A., Freeman, T.B., and Olanow, C.W. (2008). Lewy body-like pathology in long-term embryonic nigral transplants in Parkinson's disease. *Nat. Med.* 14, 504–506.
- Li, J.Y., Englund, E., Holton, J.L., Soulet, D., Haggell, P., Lees, A.J., Lashley, T., Quinn, N.P., Rehnroona, S., Björklund, A., et al. (2008). Lewy bodies in grafted neurons in subjects with Parkinson's disease suggest host-to-graft disease propagation. *Nat. Med.* 14, 501–503.
- Liu, L., Drouet, V., Wu, J.W., Witter, M.P., Small, S.A., Clelland, C., and Duff, K. (2012). Trans-synaptic spread of tau pathology in vivo. *PLoS ONE* 7, e31302.
- Luk, K.C., Song, C., O'Brien, P., Stieber, A., Branch, J.R., Brunden, K.R., Trojanowski, J.Q., and Lee, V.M. (2009). Exogenous alpha-synuclein fibrils seed the formation of Lewy body-like intracellular inclusions in cultured cells. *Proc. Natl. Acad. Sci. USA* 106, 20051–20056.
- Luk, K.C., Kehm, V., Carroll, J., Zhang, B., O'Brien, P., Trojanowski, J.Q., and Lee, V.M. (2012a). Pathological alpha-synuclein transmission initiates Parkinson-like neurodegeneration in nontransgenic mice. *Science* 338, 949–953.
- Luk, K.C., Kehm, V.M., Zhang, B., O'Brien, P., Trojanowski, J.Q., and Lee, V.M. (2012b). Intracerebral inoculation of pathological alpha-synuclein initiates a rapidly progressive neurodegenerative alpha-synucleinopathy in mice. *J. Exp. Med.* 209, 975–986.
- Mackenzie, I.R., Neumann, M., Baborie, A., Sampathu, D.M., Du Plessis, D., Jaros, E., Perry, R.H., Trojanowski, J.Q., Mann, D.M., and Lee, V.M. (2011). A harmonized classification system for FTLTDP pathology. *Acta Neuropathol.* 122, 111–113.
- Masuda-Suzukake, M., Nonaka, T., Hosokawa, M., Oikawa, T., Arai, T., Akiyama, H., Mann, D.M.A., and Hasegawa, M. (2013). Prion-like spreading of pathological alpha-synuclein in brain. *Brain* 136, 1128–1138.
- Neary, D., Snowden, J.S., Gustafson, L., Passant, U., Stuss, D., Black, S., Freedman, M., Kertesz, A., Robert, P.H., Albert, M., et al. (1998). Frontotemporal lobar degeneration: a consensus on clinical diagnostic criteria. *Neurology* 51, 1546–1554.
- Neumann, M., Sampathu, D.M., Kwong, L.K., Truax, A.C., Micsenyi, M.C., Chou, T.T., Bruce, J., Schuck, T., Grossman, M., Clark, C.M., et al. (2006). Ubiquitinated TDP-43 in frontotemporal lobar degeneration and amyotrophic lateral sclerosis. *Science* 314, 130–133.
- Nonaka, T., and Hasegawa, M. (2009). A cellular model to monitor proteasome dysfunction by alpha-synuclein. *Biochemistry* 48, 8014–8022.
- Nonaka, T., Kametani, F., Arai, T., Akiyama, H., and Hasegawa, M. (2009). Truncation and pathogenic mutations facilitate the formation of intracellular aggregates of TDP-43. *Hum. Mol. Genet.* 18, 3353–3364.
- Nonaka, T., Watanabe, S.T., Iwatsubo, T., and Hasegawa, M. (2010). Seeded aggregation and toxicity of alpha-synuclein and tau: cellular models of neurodegenerative diseases. *J. Biol. Chem.* 285, 34885–34898.
- Pesiridis, G.S., Lee, V.M., and Trojanowski, J.Q. (2009). Mutations in TDP-43 link glycine-rich domain functions to amyotrophic lateral sclerosis. *Hum. Mol. Genet.* 18(R2), R156–R162.
- Polymenidou, M., and Cleveland, D.W. (2011). The seeds of neurodegeneration: prion-like spreading in ALS. *Cell* 147, 498–508.
- Ren, P.H., Lauckner, J.E., Kachirskaja, I., Heuser, J.E., Melki, R., and Kopito, R.R. (2009). Cytoplasmic penetration and persistent infection of mammalian cells by polyglutamine aggregates. *Nat. Cell Biol.* 11, 219–225.
- Sephton, C.F., Good, S.K., Atkin, S., Dewey, C.M., Mayer, P., 3rd, Herz, J., and Yu, G. (2010). TDP-43 is a developmentally regulated protein essential for early embryonic development. *J. Biol. Chem.* 285, 6826–6834.
- Snowden, J.S., Neary, D., and Mann, D.M. (2002). Frontotemporal dementia. *Br. J. Psychiatry* 180, 140–143.
- Tsuji, H., Arai, T., Kametani, F., Nonaka, T., Yamashita, M., Suzukake, M., Hosokawa, M., Yoshida, M., Hatsuta, H., Takao, M., et al. (2012). Molecular analysis and biochemical classification of TDP-43 proteinopathy. *Brain* 135, 3380–3391.
- Wu, L.S., Cheng, W.C., Hou, S.C., Yan, Y.T., Jiang, S.T., and Shen, C.K. (2010). TDP-43, a neuro-pathogenic factor, is essential for early mouse embryogenesis. *Genesis* 48, 56–62.
- Zhang, Y.J., Xu, Y.F., Cook, C., Gendron, T.F., Roettges, P., Link, C.D., Lin, W.L., Tong, J., Castanedes-Casey, M., Ash, P., et al. (2009). Aberrant cleavage of TDP-43 enhances aggregation and cellular toxicity. *Proc. Natl. Acad. Sci. USA* 106, 7607–7612.

# Apolipoprotein E Regulates the Integrity of Tight Junctions in an Isoform-dependent Manner in an *in Vitro* Blood-Brain Barrier Model\*

Received for publication, January 27, 2011, and in revised form, March 28, 2011. Published, JBC Papers in Press, April 6, 2011, DOI 10.1074/jbc.M111.225532

Kazuchika Nishitsuji<sup>‡</sup>, Takashi Hosono<sup>‡</sup>, Toshiyuki Nakamura<sup>‡</sup>, Guojun Bu<sup>§</sup>, and Makoto Michikawa<sup>‡1</sup>

From the <sup>‡</sup>Department of Alzheimer's Disease Research, National Institute for Longevity Sciences, National Center for Geriatrics and Gerontology, Obu, Aichi 474-8522, Japan and the <sup>§</sup>Department of Neuroscience, Mayo Clinic, Jacksonville, Florida 32224

Apolipoprotein E (apoE) is a major apolipoprotein in the brain. The  $\epsilon 4$  allele of apoE is a major risk factor for Alzheimer disease, and apoE deficiency in mice leads to blood-brain barrier (BBB) leakage. However, the effect of apoE isoforms on BBB properties are as yet unknown. Here, using an *in vitro* BBB model consisting of brain endothelial cells and pericytes prepared from wild-type (WT) mice, and primary astrocytes prepared from human apoE3- and apoE4-knock-in mice, we show that the barrier function of tight junctions (TJs) was impaired when the BBB was reconstituted with primary astrocytes from apoE4-knock-in mice (apoE4-BBB model). The phosphorylation of occludin at Thr residues and the activation of protein kinase C (PKC) $\eta$  in mBECs were attenuated in the apoE4-BBB model compared with those in the apoE3-BBB model. The differential effects of apoE isoforms on the activation of PKC $\eta$ , the phosphorylation of occludin at Thr residues, and TJ integrity were abolished following the treatment with an anti-low density lipoprotein receptor-related protein 1 (LRP1) antibody or a LRP1 antagonist receptor-associated protein. Consistent with the results of *in vitro* studies, BBB permeability was higher in apoE4-knock-in mice than in apoE3-knock-in mice. Our studies provide evidence that TJ integrity in BBB is regulated by apoE in an isoform-dependent manner.

Apolipoprotein E (apoE)<sup>2</sup> is a polymorphic glycoprotein with a molecular mass of 34 kDa. Its three isoforms, apoE2, apoE3, and apoE4, are all products of the same gene, which exists as three alleles ( $\epsilon 2$ ,  $\epsilon 3$ , and  $\epsilon 4$ ) at a single locus (1). Among these three isoforms, apoE4 is a major risk factor for Alzheimer dis-

ease (AD) (2, 3). ApoE is expressed in several organs, with the liver showing the highest expression level, followed by the brain. In the brain, apoE is a major apolipoprotein and plays a major role in the transportation of lipids as a lipid acceptor (1). ApoE-containing lipoprotein particles are mainly produced by astrocytes and deliver cholesterol and other essential lipids to neurons through low density lipoprotein (LDL) receptor family members (4–6). A number of studies revealed that astrocytes are involved in the control of endothelium blood-brain barrier (BBB) properties (7, 8) and that apoE deficiency leads to BBB leakage (9–11).

BBB is formed by brain endothelial cells and is essential for the protection of the central nervous system from harmful blood molecules and cells (12). Brain endothelial cells form tight junctions (TJs), which are the fundamental characteristics of BBB (13, 14). The assembly of TJs requires at least three types of transmembrane protein, namely, occludin, claudin, and junctional adhesion molecule (15). Protein kinases are localized at TJs or interact directly with TJ proteins (16–18). Among protein kinases, PKC $\eta$  has been shown to regulate the phosphorylation of occludin at its Thr residues and play a crucial role in the assembly and/or maintenance of TJs (19). Cells surrounding brain capillaries, such as astrocytes and pericytes, contribute to the formation of a functional BBB (20). Interaction between astrocytes and brain endothelial cells is likely important for TJ formation and maintenance.

Recently, an *in vitro* BBB model in triple co-culture consisting of brain endothelial cells, pericytes, and astrocytes has been established (21). To determine whether apoE-containing particles secreted from astrocytes regulate TJ integrity in BBB, we investigated the effects of apoE isoforms on TJ integrity, using a triple co-culture model consisting of primary brain endothelial cells and pericytes, both of which were prepared from wild-type (WT) mice, and primary astrocytes prepared from human apoE3- or apoE4-knock-in mice, WT mice, or apoE-knock-out (apoE-KO) mice. Here, we provide evidence that apoE regulates PKC $\eta$  activity and the phosphorylation of occludin at its Thr residues in an isoform-dependent manner, which regulate TJ functions. The expression of occludin was not affected by either isoform. Transendothelial electric resistance (TEER), an important parameter of TJ integrity in a culture model, was lower in the model using astrocytes from apoE4-knock-in mice (apoE4-BBB model) than in the model using astrocytes from apoE3-knock-in mice (apoE3-BBB model). Consistent with the

\* This work was supported, in whole or in part, by Grants-in-aid for Scientific Research (B) 19300138 and 21300145 from the Ministry of Education, Culture, Sports, Science, and Technology of Japan (to M. M.), a grant from the Ministry of Health, Labor, and Welfare of Japan (Research on Dementia, Health and Labor Sciences Research Grant H20-007) (to M. M.), Research Funding for Longevity Sciences Grant 21-11 from the National Center for Geriatrics and Gerontology, Japan (to M. M.), National Institutes of Health Grants R01AG027924 and R01AG035355 (to G. B.), and a Zenith Fellows award from the Alzheimer Association (to G. B.).

<sup>1</sup> To whom correspondence should be addressed: Dept. of Alzheimer's Disease Research, National Center for Geriatrics and Gerontology, 35 Gengo, Morioka, Obu, Aichi 474-8511, Japan. Tel.: 81-562-46-2311; Fax: 81-562-46-8569; E-mail: michi@ncgg.go.jp.

<sup>2</sup> The abbreviations used are: apoE, apolipoprotein E; A $\beta$ , amyloid  $\beta$ ; AD, Alzheimer disease; BBB, blood-brain barrier; CM, conditioned medium; LDLR, LDL receptor; LRP, low density lipoprotein receptor-related protein; mBEC, mouse brain endothelial cell; RAP, receptor-associated protein; TEER, transendothelial electric resistance; TJ, tight junction.

results of *in vitro* studies, BBB permeability was higher in apoE4-knock-in mice than in apoE3-knock-in mice.

## EXPERIMENTAL PROCEDURES

**Materials**—A mouse monoclonal anti-LDL receptor-related protein 1 (LRP1) antibody, a rabbit polyclonal anti-LDL receptor antibody, a rabbit monoclonal anti-very low-density lipoprotein (VLDL) receptor antibody, and an anti-phosphorylated PKC $\eta$  (pPKC $\eta$ ) antibody were purchased from Abcam Inc. (Cambridge, MA). A mouse monoclonal anti-occludin antibody was purchased from Invitrogen, and a rabbit polyclonal anti-actin antibody was from Sigma. A goat polyclonal anti-apoE antibody was purchased from Millipore (Billerica, MA). Anti-phosphorylated Tyr (Tyr(P)), anti-phosphorylated Thr (Thr(P)), and rabbit polyclonal anti-PKC $\eta$  antibodies were purchased from Santa Cruz Biotechnology (Santa Cruz, CA). Mouse control IgG was from Millipore Corp. (Bedford, MA), and rabbit control IgG was from Southern Biotech (Birmingham, AL). Recombinant receptor-associated protein (RAP) was produced and purified as described previously (22, 23).

**Animals**—Mice expressing human apoE were generated by the gene-targeting technique taking advantage of homologous recombination in embryonic stem cells (knock-in) (24). Three-week-old C57BL/6 mice were purchased from SLC Inc. (Hamamatsu, Japan). For astrocyte culture, pregnant C57BL/6 mice were purchased from SLC Inc., and newborn mice at postnatal day 2 were used for the experiment. ApoE-KO mice were obtained from the Jackson Laboratories (Bar Harbor, ME). The National Center for Geriatrics and Gerontology Institutional Animal Care and Use Committee approved the animal studies.

**Evans Blue Assay**—BBB permeability was quantified using the established Evans blue dye technique. Two hundred microliters of 20% mannitol (Sigma) was injected into 6-month-old apoE knock-in mice through the tail vein. After 30 min, 200  $\mu$ l of 2% Evans blue (Sigma) was injected intraperitoneally. Mice were killed at 3 h after injection. The cerebellum and cerebral cortex were collected and then incubated in 500  $\mu$ l of formamide for 72 h in the dark. Subsequently, the absorption (*A*) of the extracted dye was measured at 630 nm by spectrophotometry.

**Cell Cultures**—Primary cultures of mouse brain capillary endothelial cells (mBECs) were prepared from 3-week-old mice in accordance with the method described previously (21). The mice were killed, and the gray matter was dissected out. The gray matter was minced in ice-cold Dulbecco's modified Eagle's medium (DMEM) (Invitrogen) and then dissociated into single cells by 25 times of up- and down-strokes with a 5-ml pipette in 10 ml of DMEM containing 100  $\mu$ l of collagenase type 2 (100 mg/ml; Sigma), 150  $\mu$ l of DNase I (1 mg/ml; Roche Applied Science) followed by digestion for 1.5 h at 37 °C. The digest in 20% bovine serum albumin (BSA) (Sigma) in DMEM was centrifuged at 1,000  $\times$  *g* for 20 min to obtain cell pellets. The microvessels obtained from the pellets were further digested with collagenase and dispase (1 mg/ml; Roche Applied Science) for 1 h at 37 °C. Microvessel endothelial cell clusters were separated on a 33% continuous Percoll (Pharmacia) gradient, collected, and washed twice in DMEM before plating on 60-mm plastic dishes coated with collagen type IV (Nitta Gelatin) and fibronectin (Calbiochem) (both 0.1 mg/ml). mBEC cultures

were maintained at 37 °C for 2 days in DMEM/F12 (Invitrogen) supplemented with mBEC medium I containing 10% FBS, basic fibroblast growth factor (1.5 ng/ml; Roche Applied Science), heparin (100  $\mu$ g/ml; Sigma), insulin (5  $\mu$ g/ml; Sigma), transferrin (5  $\mu$ g/ml; Sigma), sodium selenite (5 ng/ml; Sigma) (insulin-transferrin-sodium selenite media supplement), penicillin, streptomycin (Invitrogen), and puromycin (4  $\mu$ g/ml; Sigma). On the 3rd day, the medium was replaced with a new medium that contained all of the components of mBEC medium I except puromycin (mBEC medium II). When the cultures reached 80% confluence (4th day *in vitro*), the purified endothelial cells were passaged and used. Pure cultures of mouse cerebral pericytes were obtained by a 2-week culture of isolated brain microvessel fragments, which contain pericytes beside endothelial cells. When the cultures reached confluence, cells were treated with trypsin (Invitrogen), replated onto uncoated dishes, and cultured in DMEM supplemented with 10% FBS. Culture medium was changed every 3 days. Highly astrocyte-rich cultures were prepared in accordance with a method described previously (25). In brief, brains of day 2 postnatal human apoE-knock-in mice, WT mice, or apoE-KO mice were removed under anesthesia. The cerebral cortices from the mice were dissected, freed from meninges, and diced into small pieces; the cortical fragments were incubated in 0.25% trypsin and 20 mg/ml DNase I in PBS at 37 °C for 20 min. The fragments were then dissociated into single cells by pipetting. The cells were seeded in 75-cm<sup>2</sup> dishes with DMEM-containing 10% FBS at a density of  $5 \times 10^7$  cells/dish. After 10 days of incubation *in vitro*, flasks were shaken at 37 °C overnight, and the remaining astrocytes in the monolayer were trypsinized (0.1%) and reseeded. The astrocyte-rich cultures were maintained in DMEM-containing 10% FBS until use.

**Construction of *in Vitro* BBB Models**—To construct *in vitro* models of BBB, pericytes ( $1.5 \times 10^4$  cells/cm<sup>2</sup>) were seeded on the bottom side of the polyester membrane of the Transwell inserts (Corning Inc., Corning, NY) coated with collagen type IV and fibronectin. The cells were allowed to adhere firmly overnight, then endothelial cells ( $1.5 \times 10^5$  cells/cm<sup>2</sup>) were seeded on the upper side of the inserts placed in the wells of 24-well culture plates (for measurement of TEER) or 6-well plates (for Western blotting). Astrocytes ( $1 \times 10^5$  cells/cm<sup>2</sup>) on the 6-well plates or 24-well plates were maintained in mBEC medium II. Finally, the Transwell inserts with mBECs and pericytes were placed into the 6-well or 24-well plates with astrocytes and maintained for 7 days. For the experiment to examine the effect of apoE-containing medium on BBB integrity, the double co-cultured model using pericytes and mBECs in the absence of astrocytes was used. For the preparation of conditioned media, primary astrocytes prepared from apoE3- or apoE4-knock-in mice were cultured in mBEC medium II for 48 h, and the conditioned media of apoE3-expressing astrocytes (apoE3-CM) or apoE4-expressing astrocytes (apoE4-CM) were collected. To determine the effect of apoE3-CM or apoE4-CM on BBB integrity, each CM was added only to the luminal side of the double co-cultured model, and the abluminal side was filled with mBEC medium II. These culture media were replaced with newly prepared CM or fresh mBEC medium II on the 3rd and 5th days, and TEER was determined on the 7th day.